LARGE-SCALE TRIAXIAL TESTING OF SUSTAINABLE TDA BACKFILLING ALTERNATIVES

by

Mohammad Ashari Ghomi

Submitted in partial fulfilment of the requirements
for the degree of Master of Applied Sciences

at

Dalhousie University
Halifax, Nova Scotia
March 2018

I dedicate this thesis to my mother Zohreh, who is only supportive of my actions when I'm right but loves me even when I'm wrong.

TABLE OF CONTENTS

LIST OF TABLES

LIST OF FIGURES

ABSTRACT

One billion scrap tires are generated worldwide every year. Advanced countries have a higher rate per capita of generating scrap tires. In 2015, Canadians disposed of 37 million tires; while, nearly 250 million scrap tires were generated in the United States. The number of disposed of tires every year in Nova Scotia is equal to the number of residents. Due to environmental considerations, landfilling scrap tires is no longer allowed in Nova Scotia and stockpiling tires is not a viable option either as it is a fire hazard and a breeding ground for mosquitos and vermin. One of the most environmentally friendly methods to recycle scrap tires is to shred scrap tires into a product called Tire Derived Aggregate (TDA). While the TDA use has been on the rise recently, research on the mechanical properties of TDA is very limited.

In this research, a series of triaxial tests were conducted to evaluate the mechanical properties of TDA and TDA/soil mixtures with varying compositions of TDA and fine and coarse aggregates (i.e. TDA/sand mixtures and TDA/gravel mixtures). Each sample set was subjected to at least three different confining pressures. The results of the tests were presented and compared to the results of other researchers. Based on the tests results, empirical equations representing a number of key geotechnical properties were proposed.

LIST OF SYMBOLS USED

c	Cohesion
E_{50}	Secant modulus at 50%
R^2	Coefficients of determination
VP	Percentage of volume change
w	Ratio of the weight of the TDA to the weight of the mixture
ε	Axial strain
φ	Angle of internal friction
σ_d	Deviatoric stress
σ_3	Confining pressure
σ_e	Effective stress

ACKNOWLEDGMENTS

Sincere thanks to my supervisor, Dr. Hany El Naggar who provided valuable guidance throughout the course of this research. This thesis would not have been possible without his guidance and kind advice.

I also wish to extend my appreciation to my committee members, Dr. Craig Lake and Dr. Andrew Corkum for their helpful comments on my thesis and during the course of my research.

I would also like to thank my colleagues and friends, Jim Simmons, Ahmed Mahgoub and Yuri Martins for all their help during different stages of my research.

My gratitude also extends to Jesse Keane, Brian Kennedy and Blair Nickerson. Their assistance and technical support throughout my experimental work is greatly appreciated.

The financial support of the Natural Sciences and Engineering Council of Canada (NSERC) is gratefully acknowledged.

In addition, I gratefully acknowledge the generosity of our research collaborator, Halifax C&D Recycling Limited for the donation of all TDA materials used in this project.

CHAPTER 1 INTRODUCTION

1.1 STATEMENT OF THE PROBLEM

The number of disposed of tires every year in Nova Scotia is equal to the number of residents. Due to environmental considerations, landfilling scrap tires is no longer allowed in Nova Scotia and stockpiling tires is also not a viable option as it is a fire hazard and a breeding ground for mosquitos and vermin (Edinçliler et al., 2010). The only option left to deal with scrap tires is recycling. There are three main recycling options for scrap tires: tire derived fuel, ground rubber feed and civil engineering applications. Because of environmental considerations related to burning tires, the use of scrap tires for tire derived fuel is on the decline in North America. The use of scrap tires as ground rubber feed is increasing but only incrementally. The use of scrap tires in civil engineering applications, however, is increasing significantly (Rubber Manufacturers Association, 2016). Fig. 1.1 shows a stockpile of shredded tires.

Fig. 1.1 A stockpile of shredded tires

The main method for using scrap tires in civil engineering projects is to shred tires into small pieces referred to as tire derived aggregates (TDA). The properties of TDA must be identified in order for this product to be utilized in civil engineering projects and with the use of TDA on the rise, research has had difficulty keeping up with the demand. Conventional soil testing apparatus are not well equipped to deal with the large TDA particle sizes used in real scale civil engineering projects. Additionally, the TDA used in civil engineering projects contains steel wires, which are integral to its strength but poses an additional challenge in some laboratory testing. Due to these issues, research evaluating the properties of TDA is limited, and most of the TDA used in existing research was shredded to a smaller particle size than the TDA used in real-world applications and was free from steel wires.

1.2 BACKGROUND

Generally, TDA is manufactured by shredding or chipping scrap tires into a range of predetermined particle size distribution. This process is mechanical and commonly takes place either at ambient or cryogenic temperatures. Mechanical grinding of scrap tires at ambient temperature using cracker mills and granulators is a common practice in the industry. Alternatively, in cryogenic processing, by placing the scrap tires in liquid nitrogen, the temperature of scrap tires is brought down to below glass transition temperatures and crushed using automatic hammers (Najim & Hall, 2010).

ASTM D6270-08 specifies two standard sizes of TDA, Type A and Type B. Table 1.1 describes these two sizes. Photos of Type A and B TDA are shown in Fig. 1.2 and 1.3.

Table 1.1 TDA Type A and Type B specifications

TDA Type A	TDA Type B
Maximum dimension of 200 mm measured in any direction	Maximum dimension of 450 mm measured in any direction
100% passing the 100-mm square mesh sieve	A minimum of 90% with maximum dimension of 300 mm measured in any direction
A minimum of 95% passing the 75-mm square mesh sieve	At least one side wall shall be removed from the thread of each tire
A maximum of 50% passing the 38-mm square mesh sieve	A minimum of 75% shall pass the 200-mm square mesh sieve
A maximum of 5% shall pass the 4.75-mm square mesh sieve	A maximum of 25% shall pass the 38-mm square mesh sieve, and a maximum of 1% shall pass the 4.75-mm sieve.

Fig. 1.2 Type A TDA

Fig. 1.3 Type B TDA

1.3 OBJECTIVES OF THIS RESEARCH

In order for designers to be able to use a material, they need to know the relevant properties of that material. The amount of research to evaluate the properties of TDA and TDA soil mixtures is currently limited. To address this problem, this research is attempting to achieve the following objectives:

- To design a test scheme to evaluate the mechanical properties of TDA;
- To utilize large-scale triaxial apparatus to test the large size TDA used in the real-scale projects;
- To compare the triaxial results of varying compositions of TDA with fine and coarse aggregates (i.e. TDA/sand mixtures and TDA/gravel mixtures);
- To find empirical relationships between different key engineering parameters based on laboratory findings; and,
- To propose construction guidelines for backfill layers made of TDA;

1.4 METHODOLOGY

Before commencing the testing phase of this research, the TDA was evaluated based on ASTM D6270-08 (2012) to determine its compliance with Type A TDA standards. The TDA, gravel and sand used in this research were graded per ASTM D6913-04. The optimum moisture content for the sand and gravel used in this research was determined in accordance with ASTM D698-12. Samples were prepared using a cylindrical mould with a diameter of 152.4 mm and a height of approximately 318 mm. During sample preparation, compaction energy of 600 kJ/m^3 was used. Samples were tested using a

triaxial apparatus in consolidated drained condition. All triaxial tests were performed, and results were drawn according to ASTM D7181-11. A set of empirical equations between key parameters extrapolated from the laboratory results were derived using advanced regression techniques.

1.5 LAYOUT OF THE THESIS

The first chapter describes the research problem and lays out the objectives of this research. It also discusses the methodology of this research.

The second chapter is an extensive literature review of prior research on the subject of finding the mechanical properties of TDA. The prior research in this chapter is divided in the four categories of field research, direct shear tests, triaxial tests and other laboratory tests.

The third chapter describes the triaxial tests conducted on TDA in this research. In this chapter, the strength and stiffness properties of TDA under different confining pressures are presented. Also, empirical relationships were derived using the results of these tests.

The fourth chapter focuses on triaxial tests conducted on TDA and sand mixtures. In this chapter, the tests were conducted on five different compositions of TDA and sand. Each composition was subjected to three different confining pressures. The results for each composition are presented and discussed.

The fifth chapter discusses triaxial tests conducted on TDA and gravel mixtures. Similar to the previous chapter, the tests were conducted on five different compositions of TDA under three different confining pressures and results for each composition are discussed.

The sixth chapter compares the triaxial test results for sand, gravel and their mixtures with TDA. In this chapter, empirical equations were derived to propose a relationship between several geotechnical properties of different mixtures of TDA with sand or gravel with various TDA contents. The empirical equations were compared to laboratory results to validate their accuracy.

The seventh chapter summarizes the findings of this research and proposes future research areas and directions.

REFERENCES

Edinçliler, A., Baykal, G., & Saygili, A. (2010). Influence of different processing techniques on the mechanical properties of used tires in embankment construction. Waste Management, 30(6), 1073–1080. https://doi.org/10.1016/j.wasman.2009.09.031

Najim, K. B., & Hall, M. R. (2010). A review of the fresh/hardened properties and applications for plain- (PRC) and self-compacting rubberised concrete (SCRC). Construction and Building Materials, 24(11), 2043–2051. https://doi.org/10.1016/j.conbuildmat.2010.04.056

Rubber manufacturers association. (2016). 2015 U.S. Scrap Tire Management Summary U.S. Scrap Tire Disposition 2015, (May 2016), 1–19.

CHAPTER 2 LITERATURE REVIEW

To evaluate the mechanical properties of TDA, researchers utilized different approaches. Some researchers conducted field experiments where they used TDA in real scale projects and monitored the short and long-term deformation and stresses to deduce and back calculate the properties of TDA. Other researchers attempted to determine the properties of TDA in the laboratory utilizing a variety of methods including direct shear and triaxial testing. While direct shear testing has problems such as the predefined failure surface and limited control over confinement and saturation, triaxial testing is difficult because the steel wires present in TDA can puncture the triaxial membrane and the availability of large scale machines to accommodate the large particle size of the TDA is limited.

2.1 FIELD RESEARCH

One of the earliest TDA tests was conducted by Eaton et al. (1994). The primary goal of the study was determining the necessary thickness of tire chips to provide effective insulation from frost penetration and the minimum thickness of the overlying soil layer needed to produce a stable driving surface on a highway. This study used over 20,000 waste tires cut into 51-mm size pieces. They experimented with different thicknesses of tire shred layers, ranging from 152 to 305mm and different thicknesses of the cover soil layer from 305 to 610 mm. They observed that a 152-mm layer of tire chips could reduce frost penetration up to 25%.

Tweedie et al. (1998) built a 4.88-metre-high retaining wall test facility and instrumented the front wall to measure the horizontal stresses. By measuring the movements within the

backfill, and settlement of the backfill surface during the rotation of the wall, they were able to estimate the pattern of movement within the backfill. They compared the horizontal stresses of the tire shreds to a granular fill for a wall rotation of 0.01H and reported a 35% reduction for the tire shreds.

To study large size tire shreds (approximately 305 mm in size), Shalaby and Khan (2005) constructed a test road embankment on soft organic clay in Manitoba. Through instrumentation and performance monitoring, they concluded the following: tire shreds have a similar thermal profile to natural ground, the presence of large voids and low water content in tire shreds leads to a lower depth of frost penetration than natural clay, and one dimensional constrained compression laboratory tests can result in a good representation of the compression parameters of tire shreds. They also reported the coefficient of tire compressibility for different sizes of tire shreds and presented a simple conservative approach to interpreting the compressibility of tire shreds.

Yoon et al. (2006) constructed and instrumented a test embankment using a mixture of equal parts tire shreds and sandy soil in Lakeville Indiana. The height of the embankment was 2.1 m with a length of 20 m and a width of 17.7 m. They monitored the settlement of the road during one year of traffic, using nine settlement plates, located at three different sections of the embankment. They reported that after 200 days the settlement of the embankment was stabilized and the maximum settlement recorded was 12 mm. During the test year, they also monitored the lateral movement and the differential settlement of the embankment using vertical and horizontal inclinometers. They reported only 2 mm of relative lateral movement and no significant differential settlement.

Yi et al. (2015) conducted a series of small and large-scale one-dimensional compression tests in the laboratory as well as field tests on two types of TDA products. They investigated the influence of initial void ratio, particle size, tire source and testing method on the compressional behaviour of TDA. They constructed a test embankment consisting of two successive 20-meter-long TDA sections. To investigate the compression behaviour of TDA in the field, pressure cells and settlement plates were installed. They concluded that the compressibility of TDA depends mainly on its initial void ratio. They also mentioned that the elastic deformation of TDA is mainly controlled by the average contact area ratio of TDA particles.

Meles et al. (2014) constructed an 80-meter-long test embankment in Edmonton, AB, to investigate the compression behaviour and performance of TDA. The test embankment was constructed in four sections composed of a TDA/soil mixture, native soil and two different types of TDA for the remaining two sections. To monitor the test embankment, they used a total of 30 temperature probes and 25 settlement plates. They also conducted Falling Weight Deflectometer tests under different load levels to identify the deflection behaviour of each section after the placement of soil cover. They reported an equivalent performance between the TDA soil mixture and the conventional fill used in the control section.

The advantages of field tests are that researchers are not limited by TDA size or the presence of steel wires. In addition, by virtue of being real scale tests, they are a perfect representation of TDA at work. The disadvantages of field tests are that they are expensive, time-consuming and not practical. As a result, engineers must rely mostly on the results of laboratory tests in their designs.

2.2 LABORATORY TESTS OTHER THAN DIRECT SHEAR AND TRIAXIAL TESTS

Researchers have established a variety of different laboratory experiments to identify different geotechnical properties of soils. Some of these tests have been adapted to evaluate the geotechnical properties of TDA. Warith et al. (2004) explored the possibility of using the shredded tires in landfill leachate collection systems. They used shredded tires from two different sources to investigate the effect of the shredding process on compressibility and hydraulic conductivity. They reported that the maximum normal strain of tire shreds under compressibility tests in a confined PVC tube would plateau at the strains near 50%.

Hataf and Rahimi (2006) conducted Bearing Capacity Ratio (BCR) tests on mixtures of tire shreds and sand. In their experiment, they used rectangular shaped tire shreds with aspect ratios of 2, 3, 4 and 5 and mixture compositions of 10%, 20%, 30%, 40% and 50%. They found that the maximum BCR will occur at compositions with 40% tire shreds and an aspect ratio of 4.

To predict the compressibility behaviour of tire shreds for landfill applications, Warith and Rao (2006) performed a series of one-dimensional compressibility and permeability tests on tire shred samples. In their experiment, they predicted the required initial thickness of the tire shred layer based on the height of the waste cell. They also reported the axial strain vs. the average vertical stress and the amount of average permeability vs. the average vertical stress for their samples.

Lee and Roh (2007) performed a series of uniaxial compressive repeated loading tests on samples of recycled tire chips and expanded polystyrene. They used the results of these

tests to study the application of recycled tire chips and expanded polystyrene as cushioning material to reduce dynamic earth pressure developed during the compaction of backfills. They reported a 70% reduction in the dynamic horizontal earth pressure using recycled tire chips.

To investigate the immediate and time-dependent compression of TDA and TDA soil composites, Wartman et al. (2007) conducted a series of compression tests using an oversized oedometer and a large cantilever system. They reported an increase in the immediate compression of TDA as the TDA content and the tire particle sizes increased. They found that the tire particle size and the applied stress has a negligible effect on the time-dependent compression of TDA. They also reported that time-dependent deformation is inversely proportional to the sand content of the mixture.

To evaluate the mechanical properties of rubber-added lightweight soil, Kim and Kang (2011) performed a series of unconfined compression tests on specimens of soil with several different water and rubber contents. They reported a reduction in the unconfined compressive strength of their mixture as the rubber content increased. They also reported that the inclusion of rubber leads to the exhibition of ductile behaviour in the mixtures. They concluded that adding rubber to soil mixtures leads to low unit weight, ductile behaviour and a reduction in strength and stiffness.

Meles et al. (2014) investigated the engineering properties of TDA using a custom-made testing apparatus to perform one-dimensional compression tests. The TDA used in their tests had a variety of gradations and tire types with a maximum particle size of 300 mm. They reported engineering properties of TDA including compression behaviour, the coefficient of lateral earth pressure at rest and Poisson's ratio.

To study the dynamic performance of TDA as backfill material for retaining walls, Ahn and Cheng (2014) performed a full-scale shake table test on a retaining wall backfilled with TDA and compared the results with the conventional backfill. They reported that TDA exerted a lower amount of dynamic pressure on the wall compared to the conventional soil while causing higher amounts of displacement compared to conventional soil.

2.3 DIRECT SHEAR TESTS

Direct shear tests have been used by many researchers for their simplicity and the real-world applications of the results they provide for designers. Foose et al. (1996) conducted a series of direct shear tests on compositions of sand reinforced with shredded waste tires using a large-scale direct shear apparatus. In their study, they used three sizes of tire shreds: smaller than 50 mm, 50 to 100 mm, and 100 to 150 mm. They prepared different compositions of tire shreds and sand with 10% and 30% by volume tire shred content. Each sample was made once with a random orientation of tire shreds and again with a vertical orientation of tire shreds. They reported friction angles for their compositions. The maximum friction angle they reported was 67°, which was obtained for a composition made with larger size tire shreds and 30% tire shred content.

To evaluate the physical properties of tire sherds, Moo-Young et al. (2003) performed a set of direct shear tests on four different sizes of tire shreds. The sizes of tire shreds they used in their study were: smaller than 50 mm, 50-100 mm, 100-200 mm, and 200-300 mm. The direct shear test apparatus they used to perform their tests had a length and

width of 610 mm and a height of 305 mm. They reported a maximum friction angle of 32° for samples with 50-100 mm tire shred size.

Cetin et al. (2006) conducted direct shear tests on mixtures of tire-chips and cohesive clayey soil. In their experiments, they used two sizes of tire-chips, under 0.425 mm and 2-4.75 mm, which they called fine and coarse, but both these sizes were very small compared to industry standards. Both sizes of tire-chips were mixed with cohesive clayey soil at different weight contents of 10, 20, 30, 40 and 50%. They reported the changes in cohesion and angle of internal friction as the percentage of tire-chips changed in their mixtures.

To evaluate and compare the shear resistance of large size TDA and TDA in contact with sand, concrete and geosynthetics, Xiao et al. (2013) performed a series of large-scale direct shear tests. The TDA they used in their experiment was categorized as Type A. The dimensions of the shear box were 79 cm in width and 80 cm in length. They reported a range of 4.9 to 14.3 kPa of cohesion and a range of 18.8° to 39.3° of friction angles for their different samples. The highest cohesion they reported was for TDA on TDA while the lowest was for TDA on geotextile. The highest friction angle they obtained was for TDA on sand, and the lowest was for TDA on geogrid.

To determine the optimum mixing ratio of sand-tire chips, Reddy et al. (2015) conducted large-scale direct shear tests on different compositions of tire chips and sand. The width and length of the shear box they used were 30 cm. The tire chips they used all had the same size of 20 mm by 10 mm and the compositions they used ranged from 10% to 70% weight of the tire chips to the total mass of the mixtures. The followings are some of their conclusions: the optimum mixing ratio of sand and tire chips is in the range of 30-40% of

the total weight, and an increase of tire chips content up to 40%, can decrease the void ratio and compressibility behaviour.

El Naggar et al. (2016) performed a series of direct shear tests on different compositions of sand and TDA. In their study, they used three different sizes of TDA, dust, medium and coarse with sizes ranging from 0.5 to 48 mm. They reported: an increase in the extent of nonlinearity in the mixture as the TDA content increased; TDA content of 15% was the optimum amount as it exhibited the maximum amounts of shear resistance; and mixtures containing coarser TDA content show higher shear strength.

2.4 TRIAXIAL TESTS

While direct shear tests are simpler to perform, shortcomings such as predefined failure surface and limited control over confinement and saturation are enough to convince researchers to look for a more accurate representation of real-world circumstances. For these reasons, many researchers try to evaluate the geotechnical properties of TDA and their mixtures using triaxial testing apparatus. To evaluate the engineering properties of tire/soil mixtures, Masad et al. (1996) ran a series of triaxial tests. The tire shreds used in their experiments had a maximum size of 4.75 mm and steel wires were removed. Their samples had a diameter of only 71.1 mm and a height of 147.3 mm. They generated the following diagrams as the result of their experiment: deviatoric stress vs. axial strain; volumetric strain vs. axial strain; shear stress vs. normal stress; and elastic modulus vs. confining pressure.

Wu et al. (1997) used triaxial tests to determine the shear strength of tire chips. The tests were conducted on tire chips with sizes ranging from 2 to 38 mm and different shapes of

flat, granular, elongated and powder. Steel wires were not present in any of their tire chips. The diameter and the height of their triaxial samples were 10 and 20 cm. They determined that all their samples show a similar frictional behaviour with interparticle friction angles of 44° to 56°. They also reported a negligible amount of cohesion for confining pressures below 40 kPa.

To investigate the stress-strain relationship and strength of tire chips and their mixtures with sand, Lee et al. (1999) performed a series of consolidated drain triaxial tests. The tire chips they used had a maximum size of 30 mm and no exposed steel belting. The height of their samples was 30 cm, and the diameter of their samples was 150 mm. Their tests were conducted at confining pressures of 28, 97 and 193 kPa. They reported the results of deviatoric stress and volumetric strain vs. the axial strain and compared the results with a numerical model.

Youwai and Bergado (2003) ran a series of triaxial tests on shredded rubber tire-sand mixtures. Their samples had a diameter of 10 cm and a height of 20 cm. In their study, they experimented with different mixing ratios of rubber and sand. Due to the size limitations of their samples, the maximum size of shredded rubber tires they used was 16 mm. They reported a linear increase in the strength of the shredded rubber tire-sand mixture as the confining pressure increased. They also found that the peak internal friction angle varies from 30° to 34° with increasing sand content in the mixture.

To study the behaviour of tire shred-sand mixtures, Zornberg et al. (2004) conducted a total of 15 consolidated drained triaxial tests. In their study, they investigated the influence of tire shred content and aspect ratio on the shear strength of the mixtures. To control the aspect ratio, they cut the tire shreds into rectangular pieces with two different

widths of 12.7 and 25.4 mm. The rectangles had aspect ratios of 1, 2, 4 and the diameter of the triaxial specimens were 153 mm with a height of 305 mm. Based on their study, they reached the following conclusions: pure tire shred specimens exhibit a linear deviatoric stress vs. strain behaviour; specimens with tire shred contents lower than 35% show a dilatant behaviour while specimens with high amounts of tire shred content display contractive behaviour; and the aspect ratio of tire shred particles has a negligible effect on both volumetric strain and the stress-strain behaviour of the mixtures in strains lower than 5%.

REFERENCES

Ahn, I. S., & Cheng, L. (2014). Tire derived aggregate for retaining wall backfill under earthquake loading. *Construction and Building Materials*, *57*, 105–116. https://doi.org/10.1016/j.conbuildmat.2014.01.091

Bali Reddy, S., Pradeep Kumar, D., & Murali Krishna, A. (2015). Evaluation of the Optimum Mixing Ratio of a Sand-Tire Chips Mixture for Geoengineering Applications. *Journal of Materials in Civil Engineering*, *28*(2), 6015007. https://doi.org/10.1061/(ASCE)MT.1943-5533.0001335

Cetin, H., Fener, M., & Gunaydin, O. (2006). Geotechnical properties of tire-cohesive clayey soil mixtures as a fill material. *Engineering Geology*, *88*(1–2), 110–120. https://doi.org/10.1016/j.enggeo.2006.09.002

Eaton, R. A., Roberts, R. J., & Humphrey, D. N. (1994). Gravel Road Test Sections Insulated with Scrap Tire Chips Construction and First Year â€™ s Results aC a, (August).

El Naggar, H., Soleimani, P., & Fakhroo, A. (2016). Strength and Stiffness Properties of Green Lightweight Fill Mixtures. *Geotechnical and Geological Engineering*, *34*(3), 867–876. https://doi.org/10.1007/s10706-016-0010-1

Foose, G. J., Benson, C. H., & Bosscher, P. J. (1996). Sand Reinforced with Shredded Waste Tires. *Journal of Geotechnical Engineering*, *122*(9), 760–767. https://doi.org/10.1061/(ASCE)0733-9410(1996)122:9(760)

Hataf, N., & Rahimi, M. M. (2006). Experimental investigation of bearing capacity of sand reinforced with randomly distributed tire shreds. *Construction and Building Materials*, *20*(10), 910–916. https://doi.org/10.1016/j.conbuildmat.2005.06.019

Kim, Y. T., & Kang, H. S. (2011). Engineering Characteristics of Rubber-Added Lightweight Soil as a Flowable Backfill Material. *Journal of Materials in Civil Engineering*, *23*(9), 1289–1294. https://doi.org/10.1061/(ASCE)MT.1943-5533.0000307

Lee, H. J., & Roh, H. S. (2007). The use of recycled tire chips to minimize dynamic earth pressure during compaction of backfill. *Construction and Building Materials*, *21*(5), 1016–1026. https://doi.org/10.1016/j.conbuildmat.2006.02.003

Lee, J. H., Salgado, R., Bernal, A., & Lovell, C. W. (1999). Shredded Tires and Rubber-Sand as Lightweight Backfill. *Journal of Geotechnical and Geoenvironmental Engineering*, *125*(February), 132–141.

Masad, E., Taha, R., Ho, C., & Papagiannakis, T. (1996). Engineering Properties of Tire / Soil Mixtures as a Lightweight Fill Material. *Geotechnical Testing Journal, 19*, 297–304. https://doi.org/10.1520/GTJ10355J

Meles, D., Bayat, A., & Chan, D. (2014). One-dimensional compression model for tire-derived aggregate using large-scale testing apparatus. *International Journal of Geotechnical Engineering*, *8*(2), 197–204. https://doi.org/10.1179/1939787913Y.0000000019

Meles, D., Bayat, A., Hussien Shafiee, M., Nassiri, S., & Gul, M. (2014). Investigation of tire derived aggregate as a fill material for highway embankment. *International Journal of Geotechnical Engineering*, *8*(2), 182–190. https://doi.org/10.1179/1939787913Y.0000000015

Moo-young, H., Sellasie, K., Zeroka, D., & Sabnis, G. (2003). Physical and Chemical Properties of Recycled Tire Shreds for Use in Construction, *129*(4), 921–929.

Shalaby, A., & Khan, R. A. (2005). Design of unsurfaced roads constructed with large-size shredded rubber tires: A case study. *Resources, Conservation and Recycling*, *44*(4), 318–332. https://doi.org/10.1016/j.resconrec.2004.12.004

Tweedie, J. J., Humphrey, D. N., & Stanford, T. C. (1998). Tire Shreds as Lightweight Retaining Wall Backfill: Active Conditions. *Journal of Geotechnical and Geoenvironmental Engineering*, *124*(November), 1061–1070.

Warith, M. A., Evgin, E., & Benson, P. A. S. (2004). Suitability of shredded tires for use in landfill leachate collection systems. *Waste Management*, *24*(10), 967–979. https://doi.org/10.1016/j.wasman.2004.08.004

Warith, M. A., & Rao, S. M. (2006). Predicting the compressibility behaviour of tire shred samples for landfill applications. *Waste Management*, *26*(3), 268–276. https://doi.org/10.1016/j.wasman.2005.04.011

Wartman, J., Natale, M. F., & Strenk, P. M. (2007). Immediate and Time-Dependent Compression of Tire Derived Aggregate. *Journal of Geotechnical and Geoenvironmental Engineering*, *133*(3), 245–256. https://doi.org/10.1061/(ASCE)1090-0241(2007)133:3(245)

Wu, W. Y., Benda, C. C., & Cauley, R. F. (1997). Triaxial Determination of Shear Strength of Tire Chips. *Journal of Geotechnical and Geoenvironmental Engineering*, *123*(5), 479–482. https://doi.org/10.1061/(ASCE)1090-0241(1997)123:5(479)

Xiao, M., Ledezma, M., & Hartman, C. (2013). Shear resistance of tire derived aggregate (TDA) using large-scale direct shear tests. *Journal of Materials in Civil Engineering*, *0*(ja). https://doi.org/doi:10.1061/(ASCE)MT.1943-5533.0001007

Yi, Y., Meles, D., Nassiri, S., & Bayat, A. (2015). On the compressibility of tire-derived aggregate : comparison of results from laboratory and field tests, *458*(August 2014), 442–458.

Yoon, S., Prezzi, M., Siddiki, N. Z., & Kim, B. (2006). Construction of a test embankment using a sand-tire shred mixture as fill material. *Waste Management*, *26*(9), 1033–1044. https://doi.org/10.1016/j.wasman.2005.10.009

Youwai, S., & Bergado, D. T. (2003). Strength and deformation characteristics of shredded rubber tire - sand mixtures. *Canadian Geotechnical Journal*, *40*(2), 254–264. https://doi.org/10.1139/t02-104

Zornberg, J. G., Cabral, A. R., & Viratjandr, C. (2004). Behaviour of tire shred - sand mixtures. *Canadian Geotechnical Journal*, *41*(2), 227–241. https://doi.org/10.1139/t03-086

CHAPTER 3 STRENGTH AND STIFFNESS PROPERTIES OF TDA USING LARGE SCALE TRIAXIAL MACHINE

ABSTRACT

There is a growing interest in reusing scrap tires in civil engineering applications. Previous studies have shown that there are many promising applications for scrap tires including in highway embankments, lightweight backfills, leachate drainage for landfills, stacked bales etc. In most of these applications, scrap tires are not used directly but shredded into a product called Tire Derived Aggregates (TDA). Unlike most other civil engineering materials, TDA has not been the subject of enough experimental scrutiny to identify its physical properties and most of the experiments conducted on TDA is limited to small size TDA shreds without the presence of steel wires. This study tries to address this problem by conducting a series of consolidated drained triaxial tests on TDA using a large-scale test apparatus. The TDA used was the same TDA used in many civil engineering projects.

3.1 INTRODUCTION

Every year, approximately one billion scrap tires are generated worldwide. Advanced countries have a higher rate per capita of generating scrap tires. In the year 2015, Canadians disposed of 37 million tires (Zalando, 2016). While in the same year, nearly 250 million scrap tires were generated in the United States (Rubber manufacturers association, 2016). In the past, most of these tires were kept in stockpiles. These stockpiles were a potential environmental hazard since they were both a breeding ground

for mosquitos, vermin, rats and mice and a fire hazard (Aliabdo, Abd Elmoaty, & Abdelbaset, 2015).

By 1990 scrap tire stockpiles in the US had reached approximately a billion tires. Since then this number has been dramatically reduced through the development of new methods of reusing scrap tires. In 2015, the top three applications of scrap tires in the US were tire-derived fuel, ground rubber feed and civil engineering projects in order of use. This usage compared to 2013 represents a 9.3% decrease in tire scrap usage as tire-derived fuels, a 4.7% increase in ground rubber feed and a promising 59.8% increase in civil engineering applications (Rubber manufacturers association, 2016).

The first usage of scrap tires in civil engineering projects dates back to the mid-1980s and included using tire chips as fill and embankment material to enhance the underlying soil in highways (Tatlisoz et al., 1998). In order to include TDA in any civil engineering project as a replacement for backfilling soil materials, engineers need to know its mechanical properties. The most common tests conducted to evaluate mechanical properties of soils are the direct shear test and the triaxial test. Historically, testing equipment for geotechnical tests were designed to work with the small particles found in different types of soils. Due to the large size of TDA particles, applying these tests to TDA and TDA soil mixtures has proven problematic. To circumvent this problem, researchers tried different tactics and test methods. Some researchers relied on full-scale construction and monitoring to evaluate the properties of tire shreds and tire shred mixtures while the others used different conventional or unconventional tests for that purpose.

One of the first full-scale studies of TDA was conducted by Eaton et al. (1994). They constructed a 290-m long road with a layer of tire chips underneath to study the insulating effect of tire chips on frost penetration and observed that a 152-mm layer of tire chips can reduce frost penetration by up to 25%. Tweedie et al. (1998) built a 4.88-metre high retaining wall to test tire shreds as retaining wall backfill and compared the horizontal stress of the tire shreds at the rotation of 0.01H with the active earth pressure for a granular fill and reported a reduction 20% in horizontal stress when tire shreds were employed. Shalaby and Khan (2005) constructed a road embankment using large size tire shreds and monitored the deformation and the depth of the frost penetration. Yi et al. (2015) conducted both small-scale and large-scale laboratory compression tests and a full-scale field test on tire shreds. For their field test, they used a test road embankment to evaluate TDA as embankment fill and pavement insulation. They compared the laboratory results with field results and concluded that the elastic deformation of TDA is mainly controlled by the average contact area ratio of TDA particles. While full-scale projects give us very good examples of TDA usage, they are expensive to build and monitor and they are not feasible for most conventional projects.

Other approaches to TDA testing included Warith and Rao (2006) who performed one-dimensional compressibility and permeability tests on tire shred samples and presented strain-stress curves and the variation in the average permeability vs. the average stress. To study the applicability of tire shreds as a cushioning material to damp dynamic loads, Lee and Roh (2007) performed a series of uniaxial compressive repeated loading tests and measured the mechanical properties of tire shreds. Wartman et al. (2007) conducted compression tests on tire shreds using an oversized oedometer and a large cantilever test

system to record the immediate and time-dependent compression of TDA and reported a high degree of immediate and long-term compression for TDA. To test TDA samples with a maximum particle size of 300 mm, Meles et al. (2014) used a custom-made compression testing apparatus and reported the compression behaviour of TDA, the coefficient of lateral earth pressure at rest and the Poisson's ratio for different sample gradations. In order to test the dynamic performance of TDA as retaining wall backfill material, Ahn and Cheng (2014) compared the results of a full-scale shake table test for a wall with TDA backfill with the results of a similar shake table test with conventional fill and concluded while the amount of sliding increases, the dynamic pressure on the wall decreases significantly in a TDA backfilled wall. These tests have limited applications and do not provide enough information for design purposes in the majority of civil engineering projects.

Many researchers tried to use direct shear apparatus to evaluate the geotechnical properties of TDA. Moo-Young et al. (2003) conducted large-scale direct shear tests on TDA using an apparatus with a length and width of 600 mm. They used four different size ranges of TDA: <50 mm, 50-100 mm, 100-200 mm and 200-300 mm. They reported Mohr-Coulomb failure envelop and compressibility test results of TDA at various size ranges. Xiao et al. (2013) performed a series of large-scale direct shear tests on large size TDA and TDA in contact with sand, concrete, geogrid and geotextile. The size of TDA used was 25-75 mm, and the shear box dimensions were 79 cm wide and 80 cm long. The results were compared to sand, and the difference in failure mechanism of sand and TDA was discussed. They also reported that the range of friction angles of TDA, TDA on the sand, and TDA on concrete are about the same. El Naggar et al. (2016) performed a series

of large-scale direct shear tests on different compositions of sand and TDA mixtures. In their mixtures, they deliberately experimented with different sizes of TDA. The sizes they used were dust (width of 0.3 mm), medium TDA (width of 8.75 mm) and coarse TDA (width of 27.5 mm). They concluded that mixtures containing coarser TDA content exhibit higher shear strength and stiffness.

While direct shear tests have their benefits, there are some inherent problems such as predefined failure surface and limited control over confinement and saturation. These limitations prompted some researchers to use triaxial tests. Although triaxial tests do not have the aforementioned problems, they are difficult to perform on TDA, especially if the sample is composed of pure TDA. The size of TDA particles used in real life civil engineering projects is usually larger than the maximum particle size allowed to use in conventional triaxial machines. Furthermore, the steel wire in TDA can easily puncture the sample membrane during the test. Finally, TDA samples remain elastic in strains far surpassing soil samples, and triaxial machines have to be able to exert high strains in order for the researcher to attain any meaningful data.

Despite these challenges, a few researchers were successful at conducting triaxial tests on TDA. Masad et al. (1996) performed consolidated drained triaxial tests on tire shreds and their mixture with sand. The maximum size tire shreds they used was 4.75 mm, and the diameter of their specimens was 71.1 mm. Their specimens were subjected to confining pressures of 150, 200, 250, 300, and 350 kPa. They reported the friction angle and cohesion of TDA samples for different maximum stresses. Wu et al. (1997) conducted triaxial tests on five different shapes and gradations of TDA samples. The shapes were called Flat, Granular I, Elongated, Granular II and Powder with maximum sizes of 38, 19,

9.5, 9.5 and 2 mm respectively. The TDA they used did not contain steel wire and the diameter of their sample was 100 mm. Lee et al. (1999) presented the result of a series of consolidated drained triaxial tests on tire chips and their mixture with sand. Their samples contained TDA reinforced with steel and a maximum size of 30 mm. The diameter of their sample was 150 mm and the confining pressures used were 28, 97 and 193 kPa.

The available triaxial data on TDA in large-scale machines is limited. In addition, most triaxial tests performed on TDA used mixtures of soil and TDA. In this research, a series of consolidated drained triaxial tests were performed on TDA per ASTM D7181-11. The TDA used was the same size TDA in use in many civil engineering projects. The tests were performed using a large scale triaxial machine with a sample diameter of 152 mm (6 in) and height of approximately 2.1 times the diameter. The tests were performed on TDA with steel wire, and only the protruding part of the steel was removed to protect the membrane. In order to replicate a variety of real-world conditions, the tests were performed in a wide range of confining pressures. Through repetition, the random nature of TDA was accounted for. Finally, the results of deviatoric stress versus strain corrected for volume change are presented and discussed, and empirical equations describing key geotechnical properties are proposed.

3.2 MATERIAL

The TDA used in this research was manufactured by Halifax C&D Recycling Ltd from passenger scrap tires. The TDA complied with ASTM D6270-08 type A TDA standard. The only alteration made to the TDA was to remove the protruding part of the steel wires to protect the triaxial membrane. By removing the protruding steel, the TDA particles

cannot use the steel to lock together and it is expected that they will show less cohesion, so the results will be conservative. Sieve analyses was performed according to ASTM C136/C136M-14 with the exception of minimum sample size of 6 to 12 kg permitted per ASTM D6270-08. Fig. 3.1 displays the particle size distribution of the TDA used in this experiment. As indicated in this figure, the size of the TDA particles used was in the range of 13 mm to 63 mm.

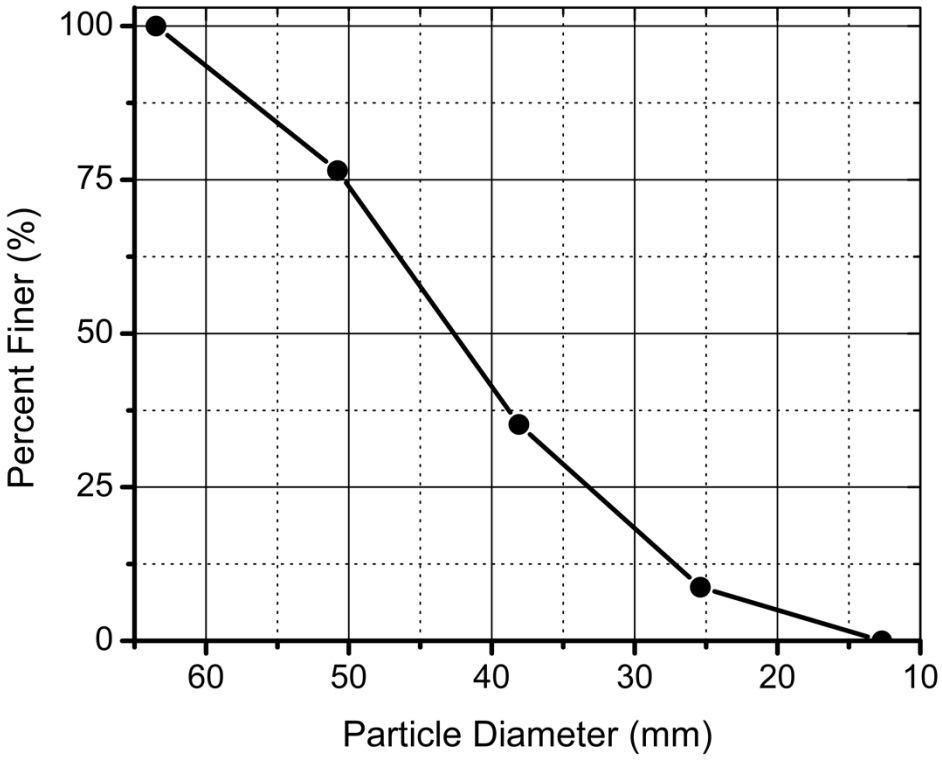

Fig. 3.1 TDA Gradation

3.3 TRIAXIAL TEST APPARATUS

A large-scale triaxial test apparatus was used in this research. The shaft of the test apparatus was extended to allow for the excessive amount of consolidation and the higher

amount of strain needed for the test. The diameter of the sample was 152 mm (6 in) and the height of the sample was around 320 mm (12.6 in) near 2.1 times the diameter and in the range permitted by ASTM D7181-11. An Instron 8501 hydraulic load frame was used for the axial loading. The load and the displacement were recorded at a frequency of 20 Hz. The displacement was set at a constant rate calculated according to ASTM D7181-11. To control the pressure and record the volume change of the sample and the cell during the test, two GDS Advanced Pressure Volume Controllers (ADVDPC) were used. Both ADVDPCs were kept at the same height and calibrated before the start of each test. The cell pressure was controlled to account for the volume change caused by the shaft movement and changes in the volume of the sample.

3.4 Sample Preparation

Before preparing the specimens, all TDA particles were checked for protruding steel wire and if present, only the protruding part of the steel wires were clipped to preserve the integrity of the membrane around the specimens. The specimens were compacted using a steel rod. As it was shown by Kowalska (2016), introducing water has insignificant influence on the dry density of TDA. Thus the specimens were kept dry during compaction. While it is permissible to perform compaction on air or oven dried TDA per ASTM D6270-08, the researchers noticed a change in physical properties of oven dried TDA and only used air drying. The dry density of all the compacted specimens was $710 \pm 5\%\ kg/m^3$. During compaction, extra care was given to protect the membrane. The membrane used was Humboldt membrane with a thickness of 0.635 mm (0.025 in) which is a relatively thick membrane. Although the researcher took these measures to protect the membrane, still more than half of the tests performed had to be repeated

because of the puncturing of the membrane. The puncturing occurred more frequently as the confining pressure increased. The only deviation from ASTM standard D7181-11 which occurred during sample preparation was that the maximum size of TDA particles were not smaller than 1/6 of the specimen diameter. However, it should be noted that this ASTM standard was developed for soil and natural aggregates and there is no existing standard for testing TDA using triaxial machines.

3.5 TESTING PROCEDURE

A total of 13 consolidated drained (CD) triaxial compression tests were performed as a part of this research. The dimensions of each specimen was measured prior to the start of the saturation stage. Because of the large particle size and high void ratio, saturation was fairly simple and fast. The B value was measured for every test, and it was always greater than 0.95. Similar to the saturation stage and for the same reasons, consolidation was relatively quick. To calculate the rate of axial loading, volume change and deformation of the specimen going through consolidation was recorded and plotted against the logarithm of elapsed time. Because of the high permeability of the specimens, the rate calculated was higher than the maximum rate that could be controlled by our ADVDPC, so the rate of 1 mm/min was chosen as the rate of axial loading. During consolidation, samples went through a considerable amount of volume change, and the shaft had to be adjusted to keep contact with the shrinking sample. The amount of volume change of the sample had a direct relationship with the confining pressure applied. Below is the equation of the best curve fitted to the volume change of the sample:

$$VP = 3.12\sigma_3^{0.39} \qquad (3.1)$$

where VP is the percentage of volume change and σ_3 is the confining pressure of the sample (kPa). Fig. 3.2 displays the amount of volume change versus the confining pressure and the fitted curve.

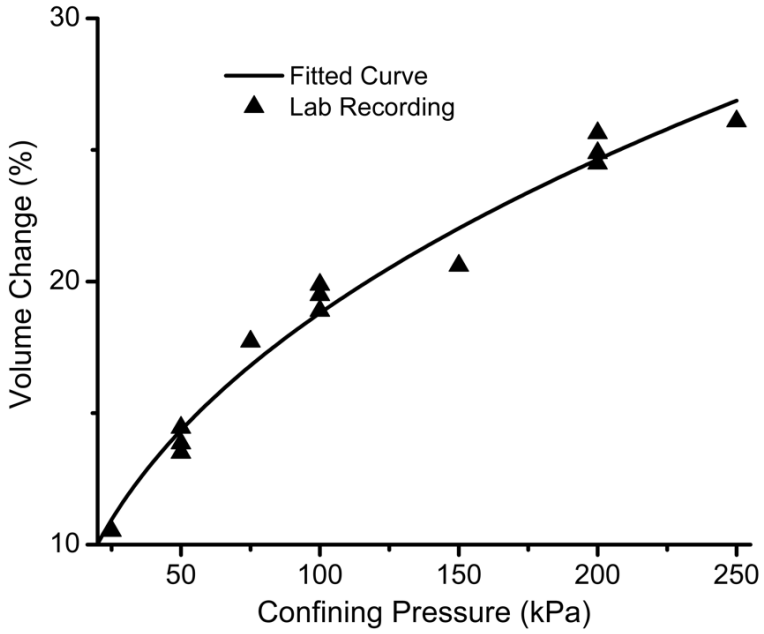

Fig. 3.2 Volume change of the sample after consolidation

During the axial loading, the amount of load, displacement as well as volume change inside the cell and the sample were recorded. Later these values were used to adjust the dimensions of the sample and calculate the amount of deviatoric stress and strain. At higher strains during the tests, specimens started to bulge visibly, and the assumption that the specimen deforms as a right circular cylinder was no longer true. It was also impossible to determine accurate values for the bulging which occurred. Because of the

elastic nature of the specimens, after unloading, they almost reverted to their original form. For this reason, the researchers did not continue the tests at strains greater than 20%.

3.6 Results and Discussion

The triaxial compression test was performed in seven different confining pressures. The confining pressures used were 25, 50, 75, 100, 150, 200 and 250 kPa. These confining pressures were chosen to resemble stress levels expected in embankments, retaining walls and shallow and deep backfills. Because of the random nature of the TDA particles and to prove repeatability, at confining pressures of 50, 100 and 200 kPa, the test was repeated three times. Fig 3.3 displays the volumetric strain versus the axial strain for different confining pressures. The changes in volume during axial loading had no meaningful relationship with the confining pressure applied and essentially showed the same trend.

The deformation which occurred in saturated soil is mainly attributed to the reorientation-rearrangement of soil particles, and the expulsion of water from the void spaces and deformation of soil particles is generally considered insignificant (Yi et al., 2015). In contrast to soil minerals, TDA particles are mainly made of rubber which exhibits near perfect elastic behaviour with Poisson's ratio of 0.5 which means the deformation of each TDA particle under load is reversible and without any change in the volume. Nevertheless, similar to the deformation of soil, TDA particles as a group can reorient and rearrange under the load to fill the void spaces available. Fig. 3.4 compares the average amount of volumetric strain recorded in this study with the amount presented by Lee et al. (1999) and Youwai and Bergado (2003). Both studies compared, used smaller

size TDA with the maximum size of 30 mm. This figure shows that the changes in volume in this study were occurring more rapidly compared to the other studies. This can be due to the larger TDA particles used in this study which can lead to more voids in the sample. These voids were being filled at a higher rate as the axial loading continued.

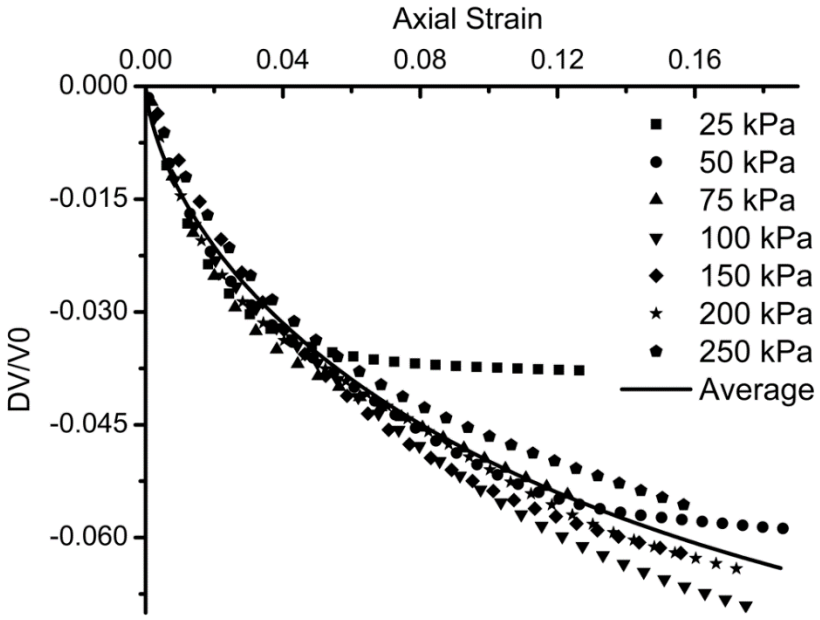

Fig. 3.3 Volumetric strain vs. axial strain

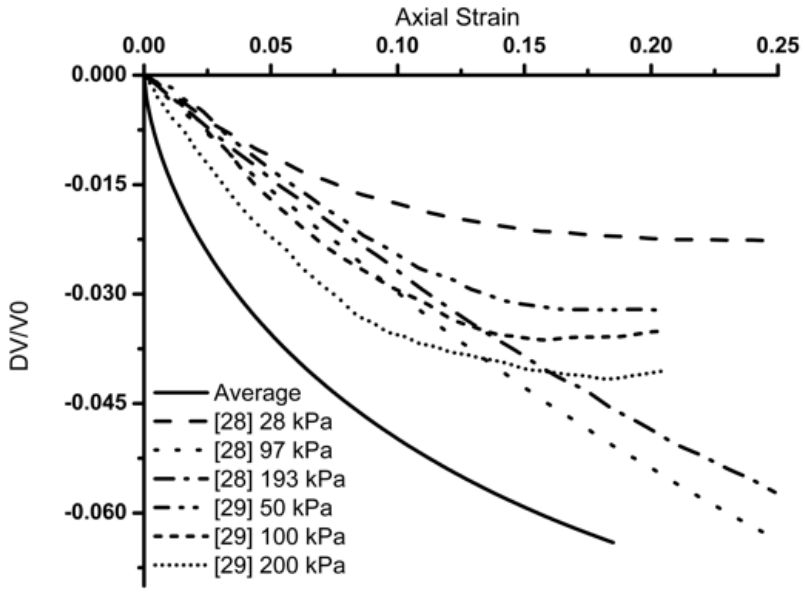

Fig. 3.4 Volumetric Strain Comparison with (J. H. Lee et al., 1999) and (Youwai & Bergado, 2003)

The random nature of the TDA particles begs the question of the repeatability of the tests performed. To tackle this question, the triaxial test was performed three times for confining pressures of 50, 100 and 200 kPa. Fig. 3.5 compares the amount of the deviatoric stress plotted against the axial strain for these tests. It is evident from the figure that the results are in strong agreement with each other. This proves the consistency of the obtained results.

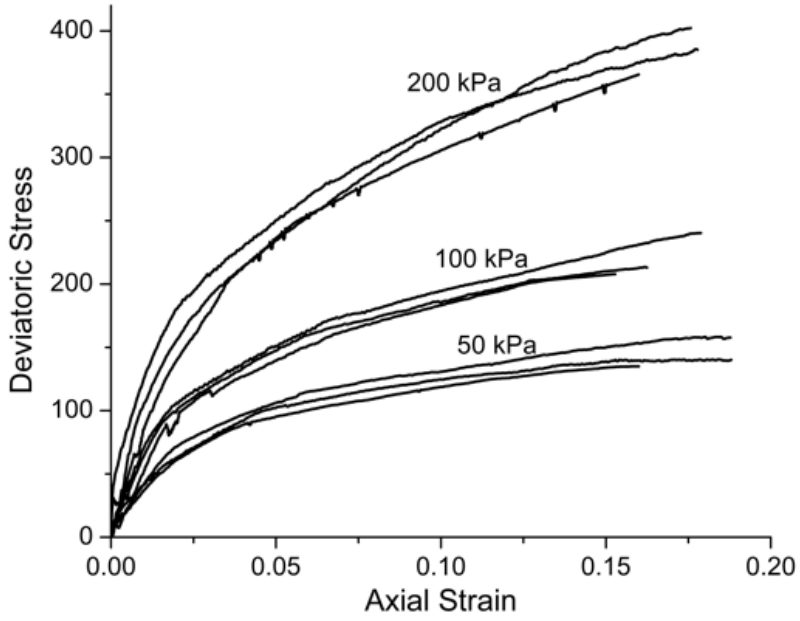

Fig. 3.5 Repeatability of the triaxial tests

3.7 STRESS-STRAIN RELATIONSHIPS

To find an imperical equation that fits the lab results, different regression methods were used for the results of each confining pressure with axial strain as the variable. The equations with two exponential terms showed the highest amount of R^2 while maintaining the simplicity. To find a reasonably simple equation that accepts both axial strain and confining pressure as input variables, the coefficients of the exponential terms were replaced with a linear line with confining pressure as the variable. Using the least squares method, the coefficients of the linear line were determined so that the R^2 for the final equation of σ is 0.9873. This procedure was repeated to fit the best equation with the amount of E_{50} calculated from the lab results. The equations below take the amount

of strain and confining pressure as input variables and calculate the amount of deviatoric strain and secant modulus (E_{50}):

$$\sigma(\varepsilon, \sigma_3) = \varepsilon[(21\sigma_3 + 2470)e^{-28.9\varepsilon} + (17.4\sigma_3 + 698)e^{-3.78\varepsilon}] \quad (3.2)$$

$$E_{50} = (7.982\sigma_3 + 778.8)e^{\left(-168.5\sigma_3^{-.03866}+98.8\right)\varepsilon_{ult}} + (30.23\sigma_3 + 2416)e^{\left(4.105\sigma_3^{-.3318}-2.129\right)\varepsilon_{ult}} \quad (3.3)$$

where σ is deviatoric stress (kPa), σ_3 is the confining pressure (kPa), ε is the amount of axial strain, ε_{ult} is the maximum strain allowed (ε_{ult} =0.15 in most applications per ASTM D7181-11) and E_{50} is the secant modulus (kPa). These equations can be used to develop material model for TDA.

Fig. 3.6 displays the deviatoric stress plotted against axial strain for different confining pressures and compares the results with the fitted curve. As it is shown in the figure, the fitted curves are in agreement with the lab results. The results indicate that the behaviour of the samples is increasingly nonlinear as the confining pressure decreases. At higher confining pressures, the results show less nonlinearity, especially at low strains.

Fig. 3.7 compares the results of this study with Youwai and Bergado (2003). While the results of Youwai and Bergado (2003) show a linear increase in the amount of deviatoric stress, the findings of this study indicate a nonlinear behaviour. Similar to the result of Youwai and Bergado (2003), Masad et al. (1996), Lee et al. (1999) and Zornberg et al. (2004) reported a fairly linear relationship between deviatoric stress and axial strain. While all these other studies show a somewhat linear behaviour for TDA's deviatoric

stress vs. strain curve, the lack of steel and the small size of the TDA particles used in these studies render their results impractical for civil engineering applications.

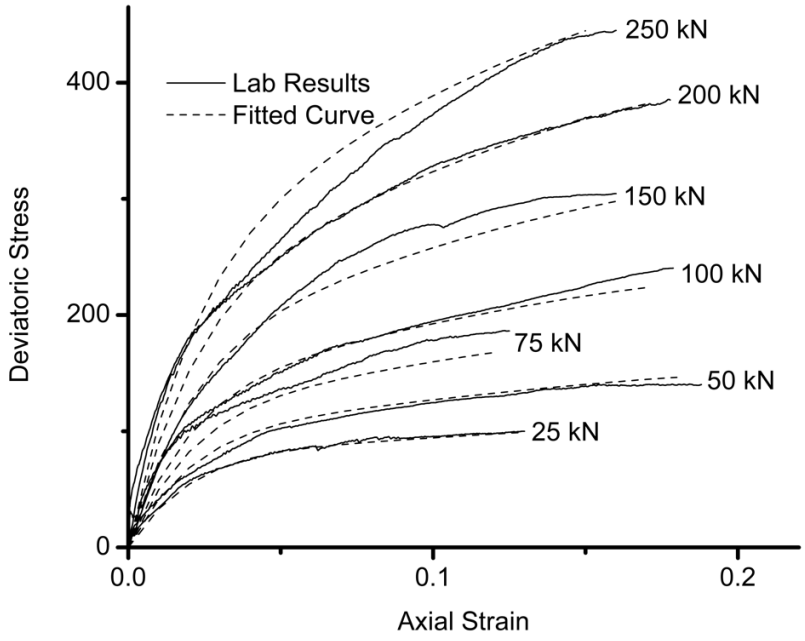

Fig. 3.6 Comparison between laboratory results and empirical equations

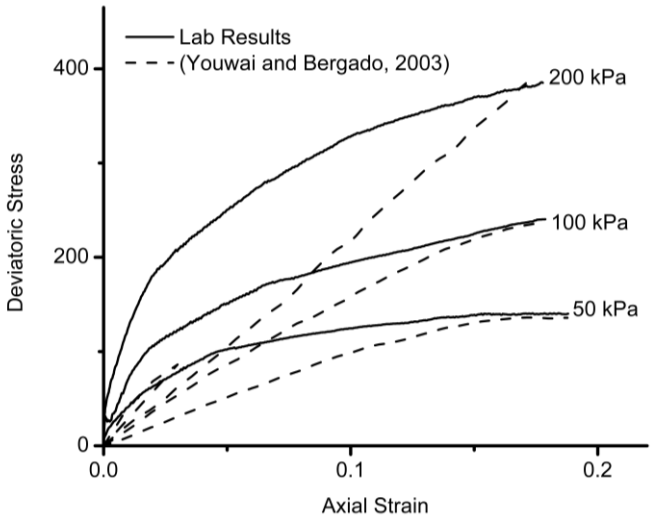

Fig. 3.7 Deviatoric Stress Comparison with (Youwai & Bergado, 2003)

While both steel and rubber present in the TDA can seperately be considered as elastic materials, the combination of steel and rubber is a more complicated material. Particularly since the particle reorientation that occurs during the axial loading can change the orientation of the steel. The presence of voids that can be filled during axial loading adds another layer of complexity to the behaviour of the specimens. These reasons can be the cause of the nonlinear behaviour observed in this investigation. On the other hand, if the steel is removed and the TDA particles used are small enough not to create a significant void volume, which was the case of most other studies, we can expect the specimens will behave linearly.

3.8 TDA Strength Parameters

As it is evident, the deviatoric stress never reached its peak maximum during the tests. ASTM D7181-11 suggests that in cases where the maximum principal stress cannot be obtained, the deviatoric stress at 15% axial strain should be considered as the maximum stress. Some researchers used the stress at 10% axial strain as their maximum stress. Depending on the strain considered, and its corresponding stress, the result of the internal angle of friction and cohesion calculated using Mohr-Coulomb failure criterion will be different. The empirical equations below are the best-fitted curve to our lab results to calculate the angle of internal friction and the cohesion:

$$\varphi = \frac{31\varepsilon_{ult}}{\varepsilon_{ult}+.032} \quad (3.4)$$

$$c = \frac{26\varepsilon_{ult}}{\varepsilon_{ult}+.016} \quad (3.5)$$

Where φ is the angle of internal friction (°), c represents the amount of cohesion (kPa) and ε is the strain considered. Plugging $\varepsilon = 0.15$ into the equations above will result in $\varphi = 25.5°$ and $c = 23.5$ kPa.

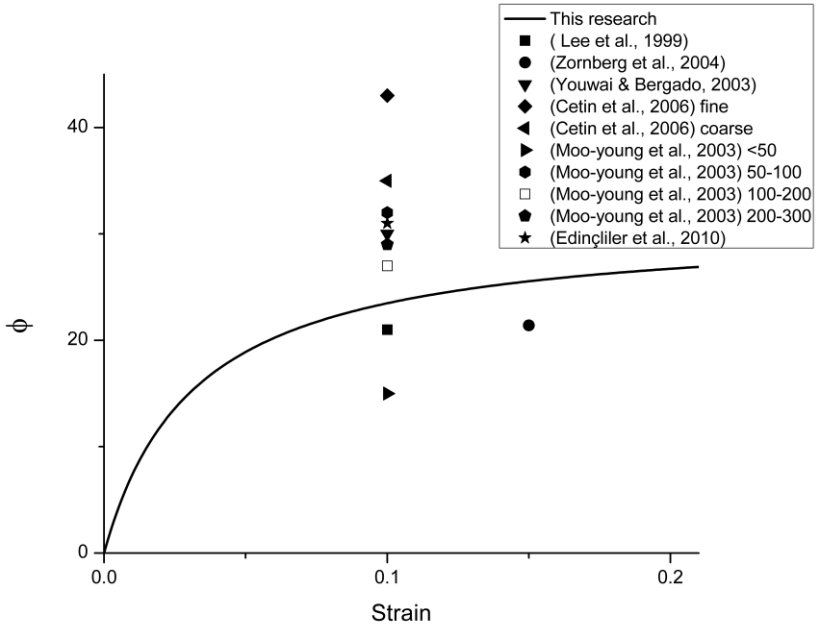

Fig. 3.8 Comparison of angle of internal friction

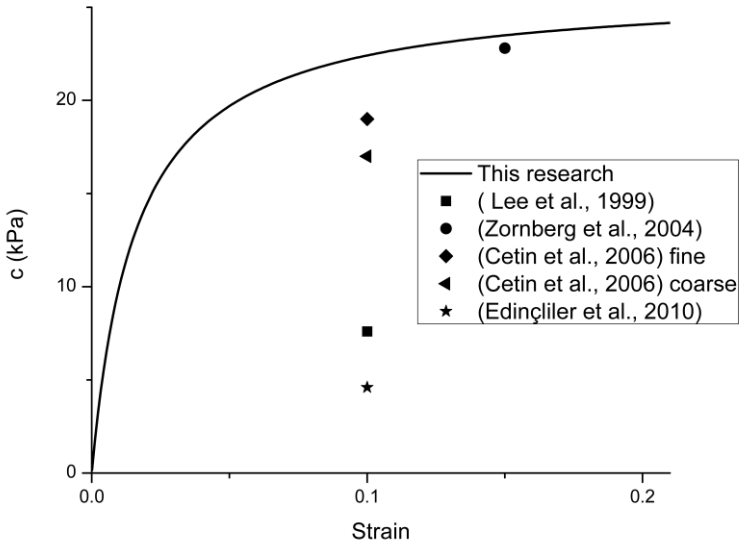

Fig. 3.9 Comparison of cohesion values

Fig. 3.8 and 3.9 compare the results of φ and c with the results obtained by other researchers. Moo-Young et al. (2003), Cetin et al. (2006) and Edinçliler et al. (2010) calculated the values φ and c based on the results of direct shear tests. Moo-Young et al. (2003) tested four different particle sizes of TDA, smaller than 50 mm, between 50 and 100 mm, between 100 and 200 mm, and between 200 and 300 mm. Cetin et al. (2006) tested two different size particles, fine with particles smaller than 0.4 mm and coarse with particle between 2 and 5 mm. Edinçliler et al. (2010) tested particles with sizes around 0.6 mm.

Lee et al. (1999), Zornberg et al. (2004) and Youwai and Bergado (2003) similar to this study, based the values of φ and c on the results of triaxial tests. The size of TDA particles used by Lee et al. (1999) was between 5 to 40 mm. Zornberg et al. (2004) used TDA particles with 12.7 mm width and four different aspect ratios. Youwai and Bergado (2003) used TDA particles sized between 4 to 13 mm.

As it is shown in the Fig. 3.9 and 3.10, there is no general agreement between the results of different researchers. The size, shape and presence of steel, as well as the type of test conducted, are a few parameters that can influence the calculated values of φ and c. The size and the shape of the TDA particles can influence the void ratio of the samples. The presence of steel can increase the stiffness of the sample and at the same time if the protruding steel wire is long enough, TDA particles can entangle with each other which can increase the amount of cohesion. And finally, the predefined failure surface and restrictions over confining pressure applied can influence the results achieved by direct shear tests.

3.9 HYPERBOLIC MODEL FOR TDA

Duncan and Chang (1970) proposed a simple, practical nonlinear stress-strain relationship which is easy to implement in finite element analysis of the soil. The advantages of their model were its simplicity and the fact that the values that are required in their model can be determined from the results of triaxial tests. The disadvantages of their model were: (1) the assumption of hyperbolic behaviour for stress-strain curves of soil which means the model cannot predict the residual strength of soil after the peak stress; (2) the model can only predict the elastic behaviour of soil and fails to predict the plastic behaviour; and (3) it only assumes that the volumetric strain of soil is compressive and cannot represent the dilatant behaviour of soils (1999). While these disadvantages limit the applications of this model for soil, since the triaxial test showed no residual strength or dilatant behaviour for TDA, this model can be a good representative of TDA behaviour.

According to the hyperbolic model:

$$\sigma = \frac{\varepsilon}{\frac{1}{E_i} + \frac{\varepsilon R_f}{\sigma_f}} \qquad (3.6)$$

where E_i is the initial tangent Young's modulus, σ_f is the deviatoric stress at failure, and R_f is the failure ratio which normally is a value between 0.5 to 0.9. The value for E_i can be calculated from below equation:

$$E_i = \frac{\partial \sigma}{\partial \varepsilon} \text{ at } \varepsilon = 0 \qquad (3.7)$$

By plugging the equation (3.2) in the above equation, the value for E_i calculated as:

$$E_i = 38.4\sigma_3 + 3168 \quad (3.8)$$

Assuming that failure occurs at ε=0.15, the value for σ_f can be calculated as below:

$$\sigma_f = 1.5217\sigma_3 + 64.2427 \quad (3.9)$$

By plugging the equations (3.8) and (3.9) in the equation (3.6) and tweaking the value of R_f to get the best fit for lab results, the value of R_f was calculated to be 0.8. This results in the below equation:

$$\sigma = \frac{\varepsilon}{\frac{1}{38.4\sigma_3+3168}+\frac{0.8\varepsilon}{1.5217\sigma_3+64.2427}} \quad (3.10)$$

Fig. 10 compares the values calculated by equation (3.10) with the laboratory results. The values calculated by equation (3.10) were close to the values of the empirical equation (3.2). As it is shown in the figure, there is a strong agreement between the results which is another indicator that the hyperbolic model suggested by Duncan and Chang (1970) is a good representative of TDA behaviour.

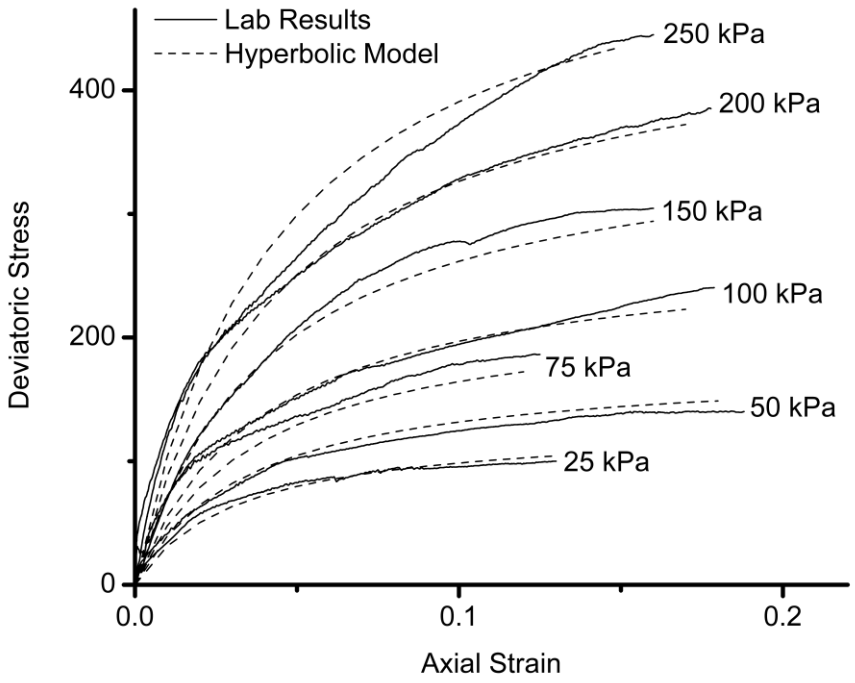

Fig. 3.10 Comparison between the hyperbolic model and the laboratory results

3.10 TDA OVERBUILD GUIDELINES

Assuming that the amount of volume change which occurs in the consolidation stage of the triaxial test is equal to the volume change which occurs in a layer of TDA buried under the ground surface, the equation below will calculate the amount of overbuild needed to reach the desired TDA layer thickness:

$$Overbuild = (TDA\ layer\ thickness) \times \left(\frac{3.12\sigma_e^{0.39}}{100-3.12\sigma_e^{0.39}}\right) \quad (3.11)$$

where σ_e(kPa) is the effective stress applied to the centre of the TDA layer. Using this equation, Fig. 3.10 displays the amount of overbuild needed to achieve different layer thicknesses. Since the thickness of TDA layers should not surpass 3 m, per ASTM

D6270-08, the figure only represents the amount of overbuild required for layers up to 3 m.

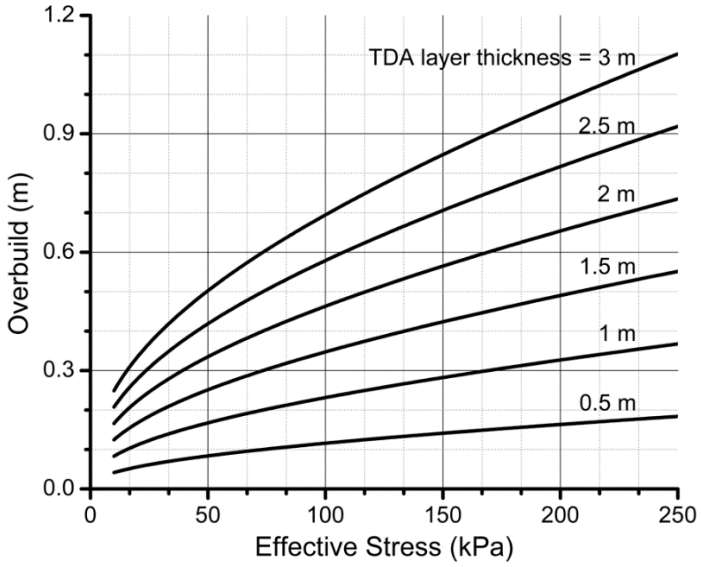

Fig. 3.11 The amount of TDA overbuild required

3.11 SUMMARY AND CONCLUSIONS

A series of consolidated drain triaxial tests were conducted on the same size TDA used in real scale civil engineering projects. All the tests were performed using a large-scale triaxial apparatus with the sample diameter of 152 mm following ASTM standards. The tests were performed in confining pressures of 25, 50, 75, 100, 150, 200 and 250 kPa. The volume change of the samples during consolidation and axial loading was recorded. The samples at higher confining pressures lose more water at consolidation stage. On the other hand, during axial loading, they show no significant difference in changes in volumetric strain. The volumetric strain of the samples during axial loading was compared to other studies, and it was shown that the larger size TDA used in the samples leads to higher amounts of volumetric strain. The amount of deviatoric stress versus

strain was presented for all the samples, and an empirical equation was proposed to fit the experimental data. To investigate the reliability and repeatability of the tests, for confining pressures of 50, 100 and 200 kPa, each test was performed three times, and the results were compared. The comparison showed an excellent level of agreement between the results which proved the repeatability of the test. Based on the test results, empirical equations were proposed for the amount deviatoric stress, secant modulus, cohesion and the angle of internal friction. Finally, based on the volume change occurred during the consolidation stage, a guideline for the amount of overbuild needed for a layer of TDA was proposed.

REFERENCES

Ahn, I. S., & Cheng, L. (2014). Tire derived aggregate for retaining wall backfill under earthquake loading. *Construction and Building Materials*, *57*, 105–116. https://doi.org/10.1016/j.conbuildmat.2014.01.091

Aliabdo, A. A., Abd Elmoaty, A. E. M., & Abdelbaset, M. M. (2015). Utilization of waste rubber in non-structural applications. *Construction and Building Materials*, *91*, 195–207. https://doi.org/10.1016/j.conbuildmat.2015.05.080

Cetin, H., Fener, M., & Gunaydin, O. (2006). Geotechnical properties of tire-cohesive clayey soil mixtures as a fill material. *Engineering Geology*, *88*(1–2), 110–120. https://doi.org/10.1016/j.enggeo.2006.09.002

Eaton, R. A., Roberts, R. J., & Humphrey, D. N. (1994). Gravel Road Test Sections Insulated with Scrap Tire Chips Construction and First Year â€™ s Results aC a, (August).

Edinçliler, A., Baykal, G., & Saygili, A. (2010). Influence of different processing techniques on the mechanical properties of used tires in embankment construction. *Waste Management*, *30*(6), 1073–1080. https://doi.org/10.1016/j.wasman.2009.09.031

El Naggar, H., Soleimani, P., & Fakhroo, A. (2016). Strength and Stiffness Properties of Green Lightweight Fill Mixtures. *Geotechnical and Geological Engineering*, *34*(3), 867–876. https://doi.org/10.1007/s10706-016-0010-1

Kowalska, M. (2016). Compactness of Scrap Tyre Rubber Aggregates in Standard Proctor Test. *Procedia Engineering*, *161*, 975–979. https://doi.org/10.1016/j.proeng.2016.08.836

Lee, H. J., & Roh, H. S. (2007). The use of recycled tire chips to minimize dynamic earth pressure during compaction of backfill. *Construction and Building Materials*, *21*(5), 1016–1026. https://doi.org/10.1016/j.conbuildmat.2006.02.003

Lee, J. H., Salgado, R., Bernal, A., & Lovell, C. W. (1999). Shredded Tires and Rubber-Sand as Lightweight Backfill. *Journal of Geotechnical and Geoenvironmental Engineering*, *125*(February), 132–141.

Masad, E., Taha, R., Ho, C., & Papagiannakis, T. (1996). Engineering Properties of Tire / Soil Mixtures as a Lightweight Fill Material. *Geotechnical Testing Journal, 19*, 297–304. https://doi.org/10.1520/GTJ10355J

Meles, D., Bayat, A., & Chan, D. (2014). One-dimensional compression model for tire-derived aggregate using large-scale testing apparatus. *International Journal of Geotechnical Engineering*, *8*(2), 197–204. https://doi.org/10.1179/1939787913Y.0000000019

Moo-young, H., Sellasie, K., Zeroka, D., & Sabnis, G. (2003). Physical and Chemical Properties of Recycled Tire Shreds for Use in Construction, *129*(4), 921–929.

Rubber manufacturers association. (2016). 2015 U . S . Scrap Tire Management Summary U . S . Scrap Tire Disposition 2015, (May 2016), 1–19.

Shalaby, A., & Khan, R. A. (2005). Design of unsurfaced roads constructed with large-size shredded rubber tires: A case study. *Resources, Conservation and Recycling*, *44*(4), 318–332. https://doi.org/10.1016/j.resconrec.2004.12.004

Tatlisoz, N., Edil, T. B., & Benson, C. H. (1998). Interaction between Reinforcing Geosynthetics and Soil-Tire Chip Mixtures. *Journal of Geotechnical and Geoenvironmental Engineering*, *124*(11), 1109–1119. https://doi.org/10.1061/(ASCE)1090-0241(1998)124:11(1109)

Tweedie, J. J., Humphrey, D. N., & Stanford, T. C. (1998). Tire Shreds as Lightweight Retaining Wall Backfill: Active Conditions. *Journal of Geotechnical and Geoenvironmental Engineering*, *124*(November), 1061–1070.

Warith, M. A., & Rao, S. M. (2006). Predicting the compressibility behaviour of tire shred samples for landfill applications. *Waste Management*, *26*(3), 268–276. https://doi.org/10.1016/j.wasman.2005.04.011

Wartman, J., Natale, M. F., & Strenk, P. M. (2007). Immediate and Time-Dependent Compression of Tire Derived Aggregate. *Journal of Geotechnical and Geoenvironmental Engineering*, *133*(3), 245–256. https://doi.org/10.1061/(ASCE)1090-0241(2007)133:3(245)

Wu, W. Y., Benda, C. C., & Cauley, R. F. (1997). Triaxial Determination of Shear Strength of Tire Chips. *Journal of Geotechnical and Geoenvironmental Engineering*, *123*(5), 479–482. https://doi.org/10.1061/(ASCE)1090-0241(1997)123:5(479)

Xiao, M., Ledezma, M., & Hartman, C. (2013). Shear resistance of tire derived aggregate (TDA) using large-scale direct shear tests. *Journal of Materials in Civil Engineering*, *0*(ja). https://doi.org/doi:10.1061/(ASCE)MT.1943-5533.0001007

Yi, Y., Meles, D., Nassiri, S., & Bayat, A. (2015). On the compressibility of tire-derived aggregate : comparison of results from laboratory and field tests, *458*(August 2014), 442–458.

Youwai, S., & Bergado, D. T. (2003). Strength and deformation characteristics of shredded rubber tire - sand mixtures. *Canadian Geotechnical Journal*, *40*(2), 254–264. https://doi.org/10.1139/t02-104

Zalando. (2016). Annual Report 2016. *Zalando Corporate Website*, 175. https://doi.org/10.1017/CBO9781107415324.004

Zornberg, J. G., Cabral, A. R., & Viratjandr, C. (2004). Behaviour of tire shred - sand mixtures. *Canadian Geotechnical Journal*, *41*(2), 227–241. https://doi.org/10.1139/t03-086

CHAPTER 4 EVALUATION OF THE PHYSICAL PROPERTIES OF TDA-SAND MIXTURES

ABSTRACT

On average, North Americans dispose of one tire per person per annum. A large portion of these discarded tires ends up in landfills which poses a major problem for the environment. One way to tackle this problem is to reuse tires in new applications. Previous studies have shown that there are many promising uses of tires in several civil engineering applications including, in highway embankments, lightweight backfills, leachate drainage for landfills, stacked bales, etc. In most of these uses, tires are shredded into a product called Tire Derived Aggregates (TDA). Despite its potential, there has not been enough experimental research done to identify the properties of TDA and TDA-soil mixtures and most of the research done is limited to small size TDA shreds to fit available small-scale triaxial machines. Other researchers used large-scale direct shear tests which have their own limitations such as predefined failure surface and limited control of confinement.

In this study, a set of tests were conducted on different TDA-soil mixtures to evaluate their physical properties. The laboratory tests conducted were performed using a large-scale triaxial machine and the TDA used were the same size as the TDA used in many real scale projects. All tests were performed following ASTM D7181-11, ASTM D6270-08, ASTM D6913-04 and ASTM D698-12 standards. Results of the triaxial tests and explanations of these results are provided.

RÉSUMÉ

En moyenne, les Nord-Américains disposent d'un pneu par personne par année. Une grande partie de ces pneus abandonnées se retrouvent dans les sites d'enfouissement, ce qui représente un majeur problème pour l'environnement. L'utilisation de ces pneus dans des nouvelles applications est un des procédés pour aborder ce problème. Des études antérieures ont montré qu'il existe de nombreuses utilisations encourageantes des pneus dans plusieurs applications de génie civil, notamment dans les remblais d'autoroutes, les talus légers, le drainage des lixiviats pour les décharges, les balles empilées, etc. Dans la plupart de ces utilisations, les pneus sont déchiquetés à un produit appelé agrégat dérivés de pneus (TDA). Malgré ses potentiels, il n'existe pas des recherches expérimentales suffisantes pour identifier les propriétés des mélanges TDA et TDA-sol. La plupart des recherches effectuées sont limitées aux déchiquetages TDA de petite taille pour s'adapter aux disponible machines triaxiales à petite échelle ou au cisaillement direct à grande échelle, limitées par la surface de défaillance prédéfinie et le contrôle de confinement.

Dans cette étude, un ensemble de tests ont été effectués sur TDA et différents mélanges TDA-sol pour évaluer leurs propriétés physiques. Les tests de laboratoire effectués ont été réalisés avec une machine triaxiale à grande échelle et le TDA utilisé était de la même taille que le TDA utilisé dans de nombreux projets à grande échelle. Tous les tests ont été effectués selon les normes ASTM D7181-11 et ASTM D6270-08. Les résultats des tests triaxiaux et les explications de ces résultats sont fournis.

4.1 INTRODUCTION

Globally, an estimated one billion tires reach the end of their lives each year. That is one tire for every seven people alive. This average is not evenly scattered. Advanced countries have a higher rate of tire consumption per population compared to third world countries. Estimates show the number of tires that will reach the end of their service life will increase to 1.2 billion by the year 2030 (Azevedo et al. 2012). In addition, there are huge stockpiles of tires all over the world. These stockpiles are both a potential fire hazard and an environmental threat. They can also provide a breeding ground for rats, mice, vermin and mosquitos (Naik and Singh 1991 and Singh 1993).

Shredding tire to Tire Derived Aggregates (TDA) and using it as a lightweight fill material in civil engineering applications such as highway embankments over soft soil has proved to be advantageous (El Naggar et al. 2016). Compacted TDA dry unit weight is less than half the average dry unit weight of soil which dramatically decreases effective stress in lower ground layers. TDA has proved to be an effective insulator for minimizing the penetration of freezing temperatures to lower frost susceptible soil layers (Yoon et al. 2006). Due to its high permeability, TDA can be used as a leachate collection layer in landfills (Warith et al. 2004). In addition, it is observed that TDA mixed with sand can enhance the engineering properties of sand (Lee et al. 1999).

Many researchers have conducted experiments to find the mechanical properties of TDA and TDA/soil mixtures using different test methods. Historically, geotechnical testing equipment is designed to deal with smaller size particles found in different types of soils. This makes the characterization of TDA relatively problematic. This problem becomes

more prominent with larger grain size tire shreds (Arroyo et al. 2007). Moo-Young et al. (2003) conducted direct shear tests in a large-scale shear box on tire shreds with gradation ranging from 50 mm to 300 mm and found a direct relationship between the increase in size and shear strength in tire shreds. Cetin et al. (2006) investigated the physical properties of fine and coarse-grained tire shreds and their mixtures with different composition of cohesive clayey soil using direct shear tests and reported different cohesion and angle of internal friction for each of their mixtures. Using direct shear tests, Arroyo et al. (2007) discussed the effect of length and sample dimension on the physical properties of TDA. Lee et al. (2014) studied the behaviour of sand-TDA mixtures at large strains using direct shear tests. El Naggar et al. (2016) explored the effect of different gradations of both TDA and sand on the shear strength of the mixture using a large-scale direct shear test apparatus.

Masad et al. (1996) conducted a triaxial test on TDA and a mixture of TDA and sand. The maximum size tire shred used in this study was 4.75 mm. Wu et al. (1997) studied the mechanical properties of five different tire shred gradations with the maximum size of 38 mm and without the presence of steel wires using 100 mm diameter triaxial apparatus. Using specimens made of tire shreds with the maximum size of 30 mm, Lee et al. (1999) carried out triaxial tests and reported the stress vs. strain curves. Youwai and Bergado (2003) investigated the effect of the sand to tire shred ratio using a triaxial testing apparatus. The sample diameter used was 100 mm, and the maximum size of the tire shred was 15 mm. Steel removed tire shreds with four different aspect ratios and a maximum particle size of 102 mm were mixed with sand and tested using a large-scale triaxial machine by Zornberg et al. (2004).

While the direct shear test is straightforward and relatively easy to perform, there are some inherent problems with this test method such as the predefined stress failure and its limited control over confining pressure. On the other hand, the size of the TDA particles and the wire embedded in them makes the use of the triaxial test machine extremely difficult. ASTM D7181-11 limits the particle size diameter to one-sixth of the sample diameter in triaxial tests which significantly limits the maximum testable gradation size. Additionally, the wire protruding from the particles can easily puncture the triaxial membrane and ruin the test results. To circumvent these problems, many researchers avoided the triaxial test and those who used this test, mostly used it on smaller size particles and removed wires which cannot be a true representation of the TDA used in the industry. In this study, a set of tests were performed on TDA/sand mixtures in accordance with the standards ASTM D7181-11 and ASTM D6270-08. The TDA used in this study was the same size TDA used in many real scale civil projects, and the wires were not removed.

4.2 MATERIAL

The TDA material used in this study was produced by our research collaborator Halifax C&D Recycling Limited which is the only tire recycling facility in Nova Scotia. The TDA used complies with the ASTM D6270-08 (2012) Type A TDA standards. Just the protruding part of the wires were removed to protect the membrane. Per ASTM D6913-04, the gradation test was performed for both the TDA and sand used in these experiments and the results are shown in Fig 4.1 and 4.2. As illustrated in Fig. 4.2, the sand used in this study is a fine graded sand. Fig. 4.3 represents the optimum water content test for the sand in accordance with ASTM D698-12.

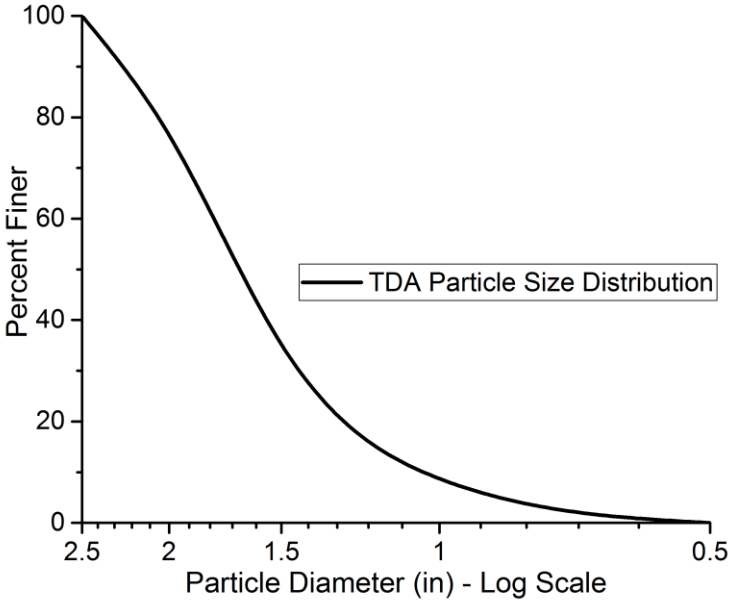

Fig. 4.1 Particle size distribution of TDA

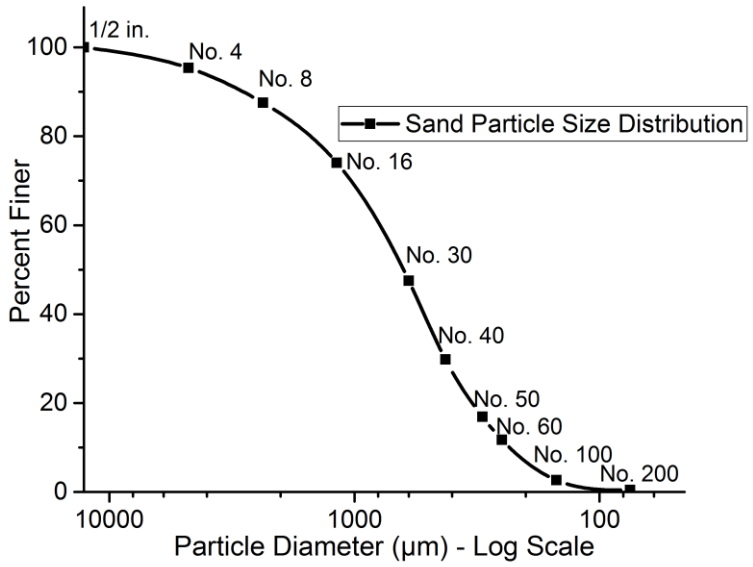

Fig. 4.2 Particle size distribution of sand

4.3 TRIAXIAL TEST APPARATUS

The tests were conducted using a large-scale triaxial test apparatus to be able to accommodate larger TDA particle sizes (see Fig. 4.4). The diameter of the samples tested was 152 mm (6 inches), and the height of the samples was approximately 318 mm (12.5 inches). The device was capable of loading the sample at high axial strains up to 35 percent. During the loading, the displacement rate was kept constant at the level specified by the ASTM D7181-11.

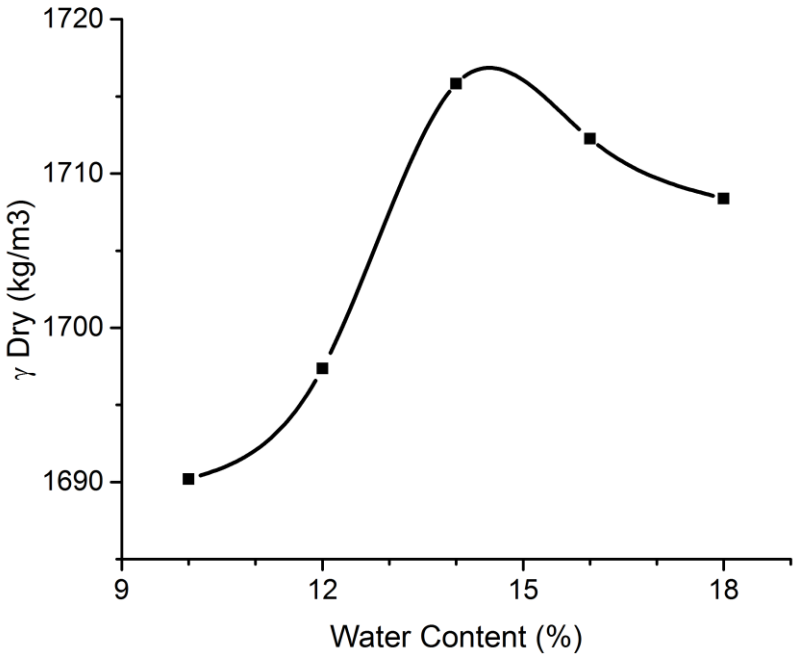

Fig. 4.3 Optimum water content of sand

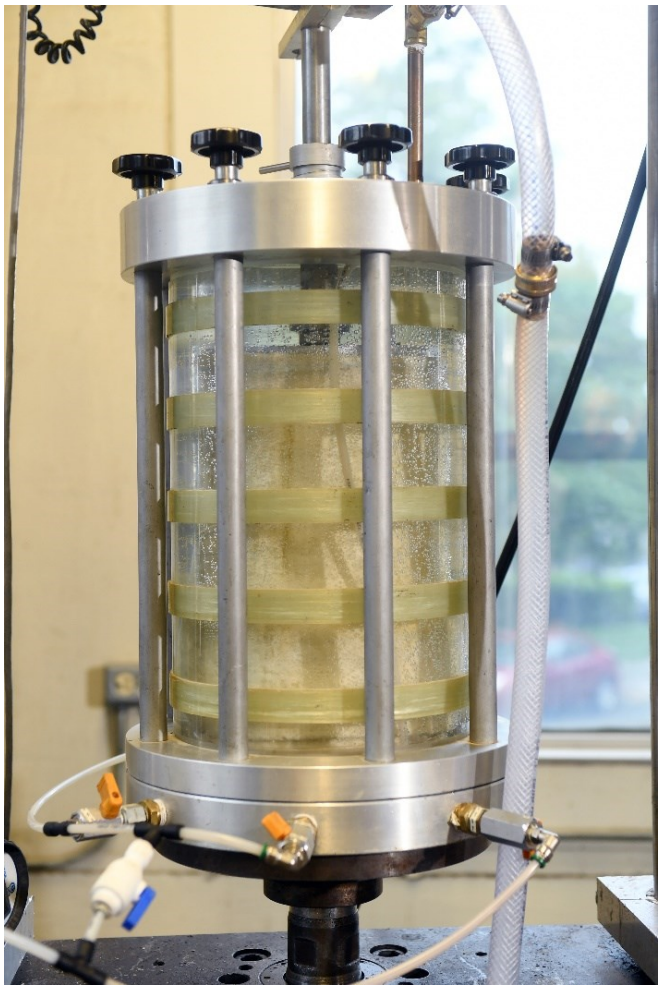

Fig. 4.4 The used large-scale triaxial apparatus

4.4 SAMPLE PREPARATION

Five sets of samples were prepared for this experiment. Each set consisted of three different samples to be tested at three different confining pressures. The sample sets consisted of one set of pure sand and four different mixture compositions of TDA and sand as illustrated in Table 4.1. Each sample was compacted using a hammer with the compaction energy of 600 kilojoules per cubic metre.

Table 4.1 Mixture properties

Composition	TDA (%) by volume	Sand (%) by volume	TDA (%) by weight	Sand (%) by weight	γ dry (kg/m^3)
Sand	0	100	0	100	1717
M15	15	85	6.4	93.6	1705
M25	25	85	11.4	88.6	1683
M50	50	50	27.8	72.2	1569
M75	75	25	53.6	46.4	1261

4.5 TESTING PROCEDURE

Each sample set was tested at three different confining pressures of 50kPa, 100kPa and 200kPa. All the tests were performed per ASTM D7181-11 standard in the consolidated drained condition. The tests were performed in three different stages of saturation, consolidation and axial loading. After the saturation stage, pore pressure parameter B was measured to ensure the elimination of air bubbles in the samples. During the consolidation stage, the volume change in the samples was plotted against time until the samples reached 100% consolidation. This plot was used to determine the maximum rate of axial loading acceptable. After this stage, axial loading started while the backpressure and the cell pressure were kept constant. During axial loading, parameters of sample length, axial load and sample volume change were recorded for later use in calculation of deviatoric stress versus strain.

4.6 RESULTS AND DISCUSSIONS

As mentioned earlier, for each of the sample sets, three tests were conducted at three different confining pressures. For each test, the deviatoric stress as plotted against strain using ASTM D7181-11 corrections for changes in length and volume. Later, using Mohr-Coulomb failure criterion, the values of cohesion and the angle of internal friction were calculated. Fig. 4.5 to 4.8 illustrate the plots of deviatoric stress vs strain for each of the mixtures of sand and TDA. For all the mixtures except M75, it can be observed that the deviatoric stress increases as the strain increase till it reaches the maximum and then it starts to decrease slowly, and after a little bit of decrease, it almost remains constant at residual stress level. In the case of M75, the triaxial machine reached its maximum possible strain and was not able to record whether the sample had a residual strength. It can be observed that in samples with lower amounts of TDA, as the confining pressure increases, the amount of maximum deviatoric stress occurs in slightly higher strains but as the percentage of TDA increases, the strain gap between the maximum deviatoric stress increases dramatically. It is also worth mentioning that the deviatoric stress for lower amounts of TDA acts more linearly.

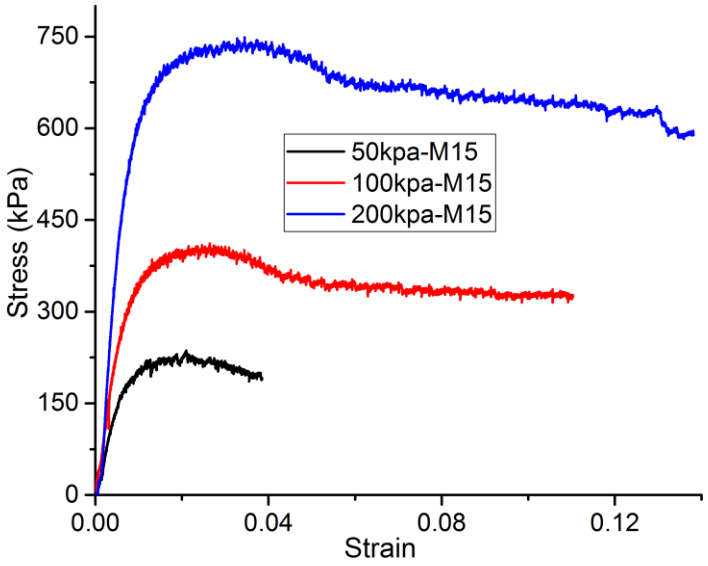

Fig. 4.5 Deviatoric stress vs. strain for M15 with three different confining pressures

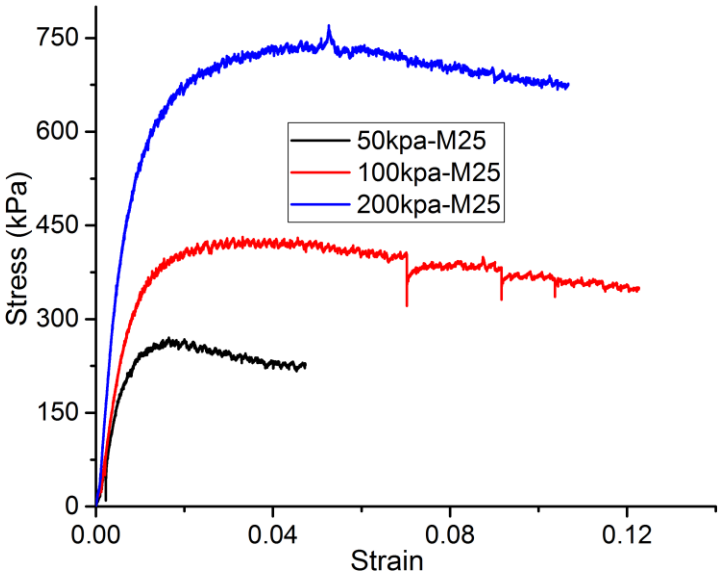

Fig. 4.6 Deviatoric stress vs. strain for M25 with three different confining pressures

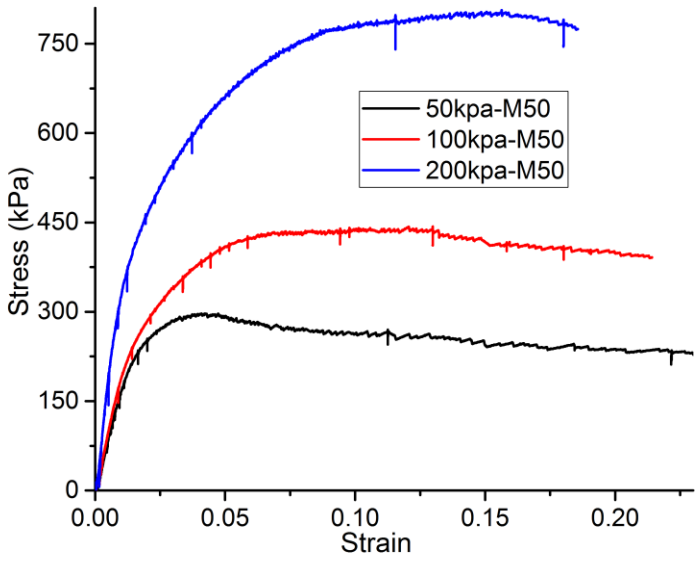

Fig. 4.7 Deviatoric stress vs. strain for M50 with three different confining pressures

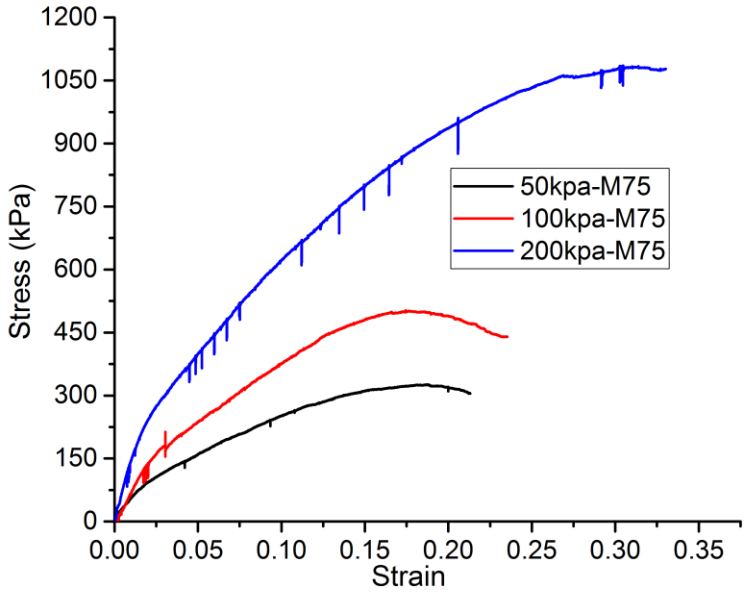

Fig. 4.8 Deviatoric stress vs. strain for M75 with three different confining pressures

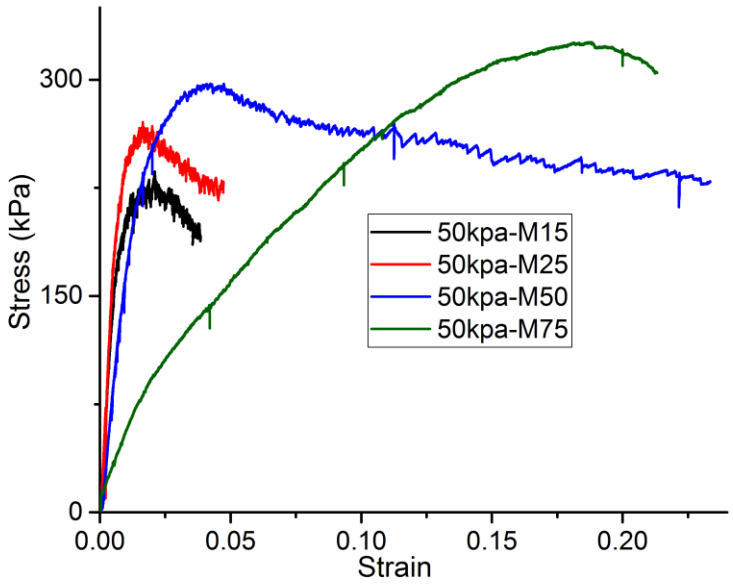

Fig. 4.9 Deviatoric stress vs. strain for different mixture at 50kPa confining pressure

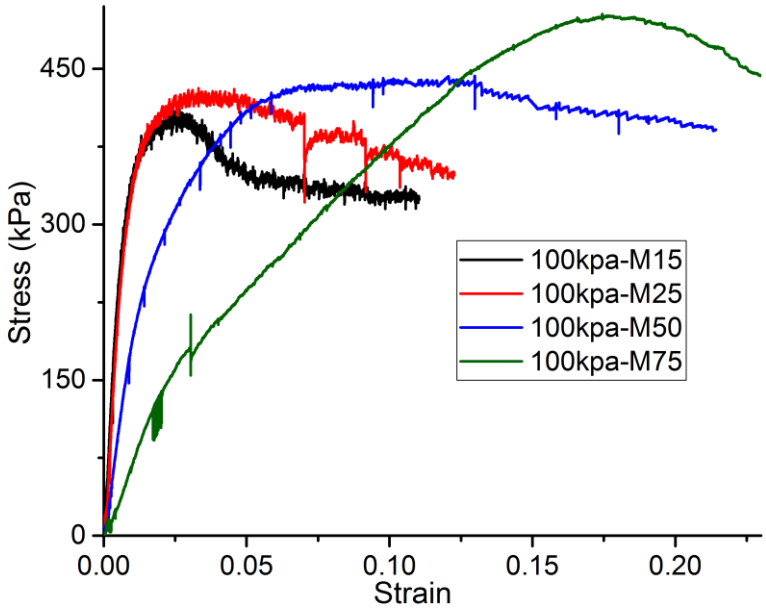

Fig. 4.10 Deviatoric stress vs. strain for different mixture at 100kPa

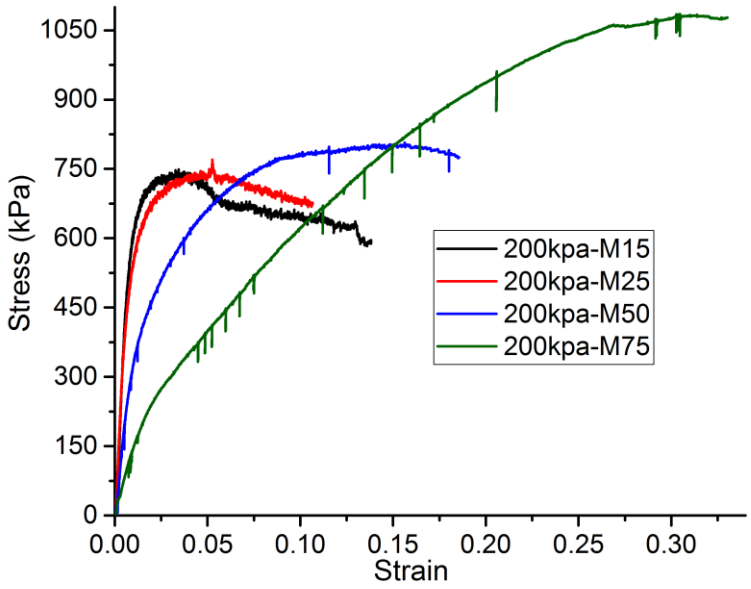

Fig. 4.11 Deviatoric stress vs. strain for different mixture at 200kPa

To compare the result of different mixtures, the deviatoric stress versus strain for different mixtures at constant confining pressure are depicted in Fig. 4.9 to 4.11. As expected, the increase in the percentage of TDA made the samples softer, and the slope of the diagram became less steep. At the same time, a small increase in the maximum deviatoric stress is observable with an increase in the percentage of TDA, but this increase becomes more significant between M50 and M75. There is also a considerable increase in the strain that maximum deviatoric stress occurs in as the percentage of TDA increases.

Fig. 4.12 depicts the volume change of different mixtures at 100kPa confining pressure. It can be observed that the behaviour of the mixture for lower percentages of TDA is like

the behaviour of dense sand but as the percentage of TDA increases, the behaviour more closely resembles the behaviour of loose sand.

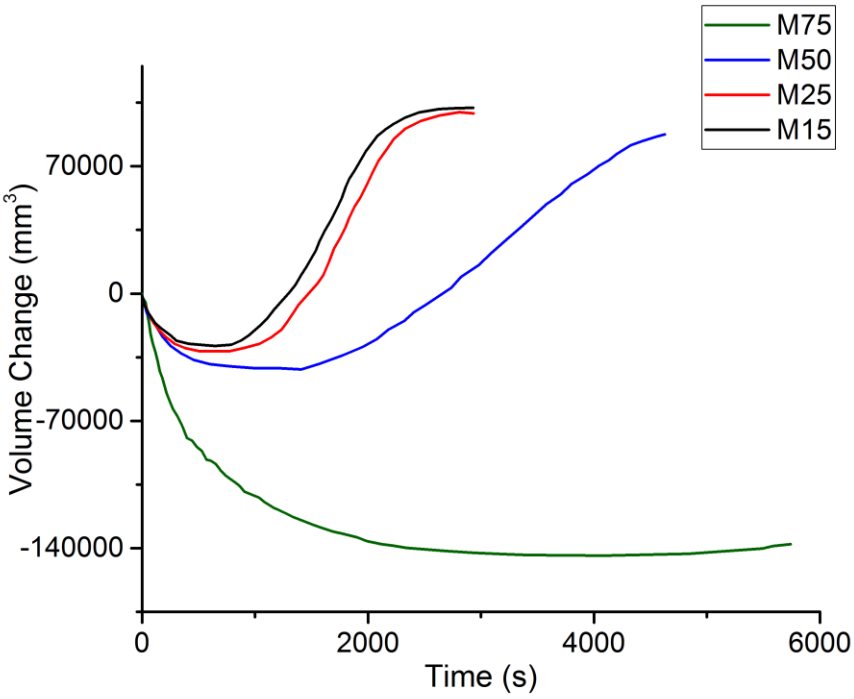

Fig. 4.12 Volume change over time for different mixtures at 100kPa

The values for cohesion and the angle of internal friction of different mixtures are provided in Table 4.2. According to these values, while the amount of φ is relatively constant, the value of cohesion increases by the increase in the percentage of TDA. It should be noted that the strength parameters presented in table 2 represent the ultimate limit state which occurred at strain levels of 2% to 5% for mixtures M15 and M25 and up to strain levels of 15% to 25% for the other two mixtures (i.e., M50 and M75).

Table 4.2 The amount of cohesion and the angle of internal friction for different mixtures

Composition	Cohesion (kPa)	The angle of internal friction (φ)
Sand	10.9	39
M15	15.4	39
M25	29.7	38
M50	32.3	39
M75	36	40

4.7 CONCLUSIONS

Using the same size TDA as the TDA used in real scale civil engineering projects, a set of tests were conducted on different TDA-soil mixtures, and the results were presented. All the tests were conducted using a large-scale triaxial machine following ASTM D7181-11, ASTM D6270-08, ASTM D6913-04 and ASTM D698-12 standards. The changes occurred in deviatoric stress caused by the changes in confining pressure and the percentage of TDA in the mixture were discussed. In the end, the values for the cohesion and the angle of internal friction were presented for all considered mixtures. It was noted that the value of φ was relatively constant, whereas the value of cohesion increases with the increase in the TDA percentage.

ACKNOWLEDGMENT

The authors acknowledge the financial support provided by the Natural Sciences and Engineering Research Council of Canada (NSERC), and the generosity of our research collaborator Halifax C&D Recycling Limited for the donation of all TDA materials used in this project.

REFERENCES

Arroyo, M., Estaire, J., Sanmartin, I. and Lloret, A., 2007, November. Size effect on tire derived aggregate mechanical properties. In *Scrap Tire Derived Geomaterials-Opportunities and Challenges: Proceedings of the International Workshop IW-TDGM 2007 (Yokosuka, Japan, 23-24 March 2007)* (p. 151). CRC Press.

Azevedo, F., Pacheco-Torgal, F., Jesus, C., de Aguiar, J.B. and Camões, A.F., 2012. Properties and durability of HPC with tyre rubber wastes. *Construction and building materials*, *34*, pp.186-191.

Cetin, H., Fener, M. and Gunaydin, O., 2006. Geotechnical properties of tire-cohesive clayey soil mixtures as a fill material. *Engineering geology*, *88*(1), pp.110-120.

El Naggar, H., Soleimani, P., & Fakhroo, A. (2016). Strength and Stiffness Properties of Green Lightweight Fill Mixtures. *Geotechnical and Geological Engineering*, *34*(3), 867-876.

El Naggar, H., Soleimani, P., & Fakhroo, A. (2014). Strength and Stiffness Properties of Lightweight TDA-Sand Fill Mixtures. 67th *Canadian Geotechnical Conference*, Regina, Saskatchewan, Canada.

Lee, C., Shin, H. and Lee, J.S., 2014. Behavior of sand–rubber particle mixtures: Experimental observations and numerical simulations. *International Journal for Numerical and Analytical Methods in Geomechanics*, *38*(16), pp.1651-1663.

Lee, J.H., Salgado, R., Bernal, A. and Lovell, C.W., 1999. Shredded tires and rubber-sand as lightweight backfill. *Journal of Geotechnical and Geoenvironmental Engineering*, *125*(2), pp.132-141.

Masad, E., Taha, R., Ho, C. and Papagiannakis, T., 1996. Engineering properties of tire/soil mixtures as a lightweight fill material.

Moo-Young, H., Sellasie, K., Zeroka, D. and Sabnis, G., 2003. Physical and chemical properties of recycled tire shreds for use in construction. *Journal of environmental engineering*, *129*(10), pp.921-929.

Naik, T.R. and Singh, S.S., 1991, January. Utilization of discarded tires as construction materials for transportation facilities. In *70th Annual Meeting of Transportation Research Board*.

Singh, S.S., 1993.. *Wisconsin Professional Engineer*, pp.14-17.

Warith, M.A., Evgin, E. and Benson, P.A.S., 2004. Suitability of shredded tires for use in landfill leachate collection systems. *Waste Management*, *24*(10), pp.967-979.

Wu, W.Y., Benda, C.C. and Cauley, R.F., 1997. Triaxial determination of shear strength of tire chips. *Journal of geotechnical and geoenvironmental engineering*, *123*(5), pp.479-482.

Yoon, S., Prezzi, M., Siddiki, N.Z. and Kim, B., 2006. Construction of a test embankment using a sand–tire shred mixture as fill material. *Waste Management*, *26*(9), pp.1033-1044.

Zornberg, J.G., Cabral, A.R. and Viratjandr, C., 2004. Behaviour of tire shred sand mixtures. *Canadian Geotechnical Journal*, *41*(2), pp.227-241.

CHAPTER 5 SUSTAINABLE MIXTURES OF TDA AND CLASS A GRAVEL

ABSTRACT

Stockpiling or landfilling discarded tires poses significant problems for the environment. In order to address these problems, several methods are currently employed to reuse discarded tires. One of these methods, which is gaining popularity, is to shred discarded tires into tire derived aggregates (TDA) and use them in civil engineering purposes such as backfill material for embankments or foundations. Despite the recent popularity of TDA, the experimental research to identify its geotechnical properties is limited or non-existent. Furthermore, most of the research done was either with small size TDA particles, to accommodate the readily available small-scale triaxial machines, or used direct shear apparatus which has limitations such as predefined failure surface and limited control over confinement pressure. In this study, the physical properties of five different TDA-gravel mixtures were evaluated using a large-scale triaxial machine. The TDA used in this study was the same size TDA used in civil engineering projects. All the tests were conducted according to ASTM standards. Finally, the results of deviatoric stress and volumetric strain vs axial strain for each mixture was reported and discussed.

***Keywords*:** Triaxial test; TDA; Tire derived aggregates; Tire shred; Gravel; Deviatoric stress; Volumetric strain

5.1 INTRODUCTION

Advances in the industry and growing population has led to an increase in the number of scrap tires produced every year. In the year 2015, Canadians disposed of 37 million tires (Zalando, 2016) while 250 million scrap tires were disposed of in the US (Rubber manufacturers association, 2016). Stockpiling scrap tires can be dangerous. Stockpiles can be a potential fire hazard or a breeding ground for rats, mice or mosquitos (Ashari, et al., 2017). Reusing scrap tires prevents these environmental risks, averts depletion of the natural resources and gives them ecological value. The top three applications of scrap tires are tire-derived fuels, ground rubber feed and civil engineering projects respectively. Compared to the other applications, using scrap tires in civil engineering projects has recently shown the most amount of growth (Rubber manufacturers association, 2016). To use scrap tires in civil engineering applications, they must be shredded into TDA first. Despite the recent growth in TDA usage, there is not enough experimental research to identify its mechanical properties. Additionally, most of the research done on TDA is not representative of the TDA used in civil engineering applications. The larger particle size of the TDA used by the industry is difficult for researchers to use in experiments. In addition, the existence of steel belts in TDA can further complicate experiments. For these reasons, in the past, most researchers either removed the steel belts and shredded the TDA to smaller sizes or ran other types of less accurate tests on TDA.

Many researchers have tried to use direct shear tests to evaluate the geotechnical properties of TDA and TDA mixed with soil. Foose et al. (1996) conducted direct shear tests on different mixtures of dry sand and shredded tires. In their study, the dried sand was mixed with three different categories of length of wire reinforced tire shreds: smaller

than 5 cm, 5 to 10 cm and 10 to 15 cm. The tests were conducted for 10% and 30% tire shred content by volume, and they used both vertical and random orientations of tire shreds. For their tests, they used a large-scale direct shear machine and reported the maximum shear strength, vertical displacement and friction angles of their specimens. Tatlisoz et al. (1998) used a large-scale direct shear machine and tested different compositions. The lengths of tire chips used in their experiment were between 30 to 110 mm. The compositions consisted of pure tire chips, sand, silty sand and mixtures of tire chips with either sand or silty sand at 10, 20 and 30 percent by volume. They reported the amounts of maximum shear strength, cohesion and the internal friction angle for their specimens. To investigate the geotechnical properties of tire shreds and tire shreds mixed with a cohesive clayey soil, Cetin et al. (1998) performed direct shear tests on tire shreds and their mixtures with different composition of cohesive soil. The tire shreds that they used were free of steel belts and fine in size with the maximum size of 4.75 mm. To study the effect of TDA particle size on shear strength and stiffness of TDA/sand mixtures, El Naggar et al. (2016) performed a series of large-scale direct shear tests on different compositions of sand and TDA mixtures. Their results show that mixtures with coarser TDA content possess higher amounts of stiffness and shear strength.

Some researchers used triaxial tests to study TDA and TDA/soil mixtures. Masad et al. (1996) used a small-scale triaxial machine to evaluate the engineering properties of tire/soil mixtures. The diameter of their samples was 71.1 mm, and the maximum tire chips size that they used was 4.75 mm. The steel belts were not present in their experiment. They reported the friction angle and cohesion of their compositions. To investigate the stress versus strain relationship and the strength of tire chips mixed with

sand, Lee et al. (1999) conducted a triaxial testing program. In their experiment, they used tire chips with a maximum size of 30 mm with no exposed steel belts. They reported the mechanical properties of their composition. Utilizing a large scale triaxial apparatus, Zornberg et al. (2004) performed a total of 15 consolidated drained triaxial tests with samples made of tire shred- soil mixtures. In their experiment, they used rectangular shaped tire shreds from which the steel had been removed. The diameter of their specimens were 6 inches and they used three confining pressures of 48.3, 103.5 and 207 kPa and reported the results. Noorzad and Raveshi (2017) performed a series of consolidated drained triaxial tests on mixtures of sand and tire crumbs. The TDA used was devoid of steel and with a maximum particle size of about 5 mm. They reported the amount of cohesion and the angle of internal friction for their mixtures.

5.2 MATERIAL

The gravel and TDA used in this experiment were graded according to the ASTM standard. The gravel used in the experiment was Type 1 gravel per Nova Scotia Transportation and Public Works Standard Specification. The particle size distribution of the gravel is shown in Fig. 5.1a The TDA used was shredded and manufactured by Halifax C&D Recycling Ltd from discarded passenger tires. The TDA was tested for size gradation and metal fragments and it complied with Type A TDA per ASTM D6270-08 standard. Fig. 5.1b depicts the TDA particle size distribution used in this experiment. As evident from the figure, the size of the TDA particles was in the range of 13-63 mm. To protect the triaxial membrane, the protruding part of the steel wires were removed from the TDA particles. Removing the protruding steel can diminish the ability of TDA particles to interlock during the test which can decrease the cohesion of the samples. Fig.

5.2 represents the results of the optimum water content test for the gravel in accordance with ASTM D698-12.

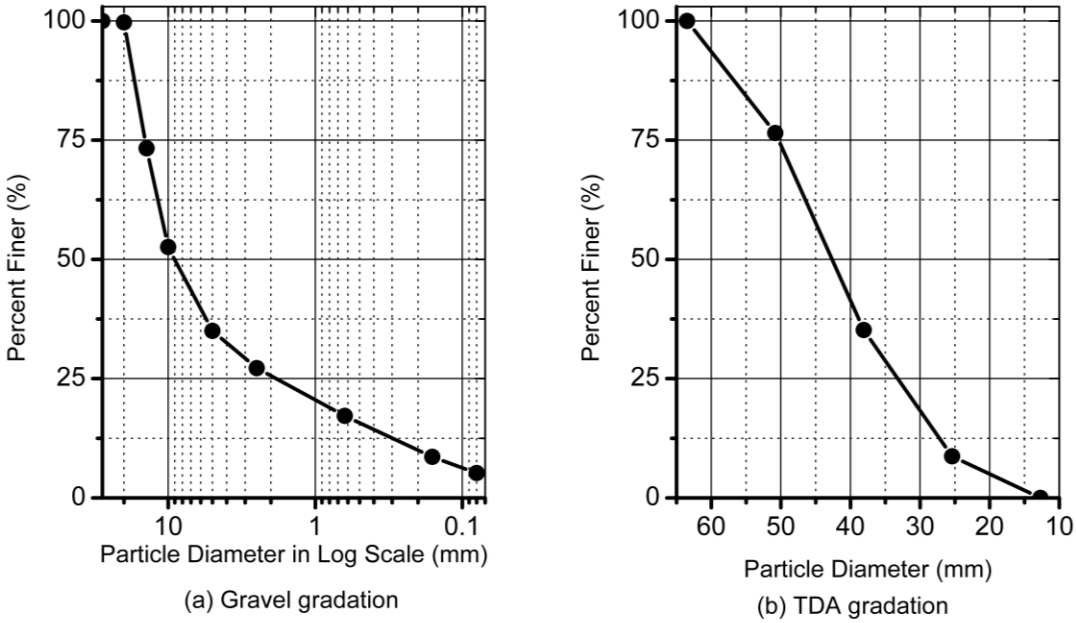

Fig. 5.1 Particle size distributions of gravel and TDA

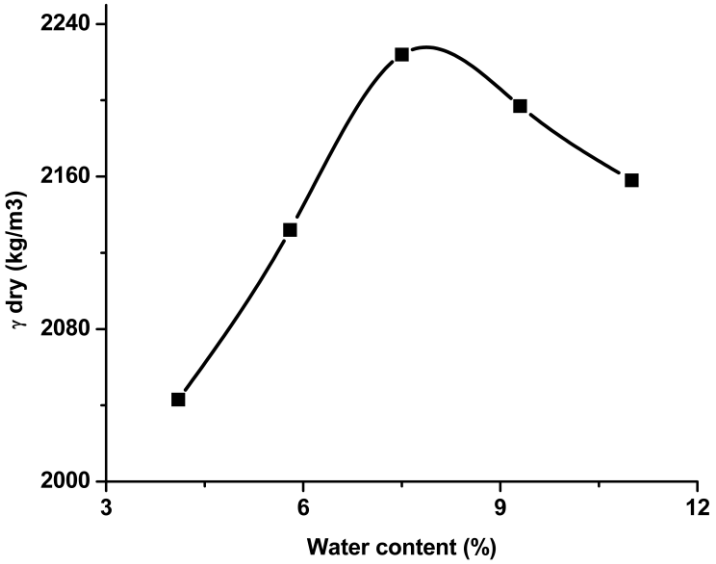

Fig. 5. 2 Optimum water content of Gravel

5.3 TRIAXIAL TEST APPARATUS

All triaxial tests in this research were conducted using a large-scale triaxial apparatus capable of testing samples of 152 mm in diameter. In order to apply the axial loading an Instron 8501 hydraulic load frame, capable of recording the load and displacement at a frequency of 20 Hz, was used. Two GDS Advanced Pressure Volume Controllers were utilized to record the volume change of the sample and cell while keeping the pressure constant.

5.4 SAMPLE PREPARATION

Five sets of samples with different compositions were prepared. Each set included three samples to be tested under three different confining pressures. The sample sets consisted of one set of 100% gravel as the reference case and four different compositions of gravel and TDA as shown in Table 5.1. Before compaction, water was added to the gravel to reach optimum moisture content. All samples were compacted with the compaction energy of 600 kilojoules per cubic metre using a standard Proctor.

Table 5.1 Mixture properties

Composition	TDA (%) by weight	Gravel (%) by weight	Dry density (kg/m^3)
Gravel	0	100	2108
M5	5	95	1815
M10	10	90	1749
M20	20	80	1593
M30	30	70	1483

5.5 Testing Procedure

All the tests were performed in consolidated drain condition according to ASTM D7181-11. Each sample set was tested at three different confining pressures of 50kPa, 100kPa and 200kPa. According to the standard, tests were performed in three stages of saturation, consolidation and axial loading. During the saturation stage, the parameter of pore pressure B was measured to make sure that the amount of air bubbles in the sample was insignificant. Throughout the consolidation stage, the amount of volume change in the sample was recorded and plotted against time. Later this plot was used to calculate the maximum rate of axial loading per ASTM standard. After the completion of the consolidation stage, the samples were subjected to axial loading. During axial loading, the amount of load, deformation and volume change inside the sample and the cell were recorded. Later these values were used to calculate and draw the deviatoric stress versus strain curves.

5.6 Results and Discussions

As mentioned, for each sample during the axial loading, the volume changes inside the sample were recorded. Using these changes in volume, the amount of volumetric strain of the sample was calculated and plotted against the axial strain in Fig. 5.3. As shown in the figure, the volumetric strain in the samples with a lower amount of TDA resembles the gravel which is to be expected. On the other hand, as the percentage of TDA increases, this resemblance diminishes. Additionally, in samples with a lower amount of TDA,

confining pressure influences volumetric strain. However, this influence reduces as the percentage of TDA increases. This can be seen more prominently in M30 samples which behave similarly to the pure TDA sample.

The results of deviatoric stress versus strain for all the sample sets at confining pressures of 50kPa, 100kPa and 200kPa are plotted in Fig. 5.4. The ASTM correction for changes in length and volume were applied when plotting the graphs. It can be seen that for all samples except M30, after the deviatoric stress reaches a peak amount, it starts decreasing gradually. In other words, as the percentage of TDA increases, the sample behaviour shifts from pure gravel behaviour towards pure TDA behaviour which is to be expected. It is possible that if the test were continued beyond the strain of 20%, the deviatoric stress would have reached a peak maximum but continuing the test was beyond the capabilities of the triaxial apparatus. Even reaching these high amounts of strain required tweaking the triaxial machine and extending the axial loading shaft. Fig. 5.5 compares the results of deviatoric stress versus strain for different mixtures. It is evident that as the percentage of TDA increases, the curves become less steep. That is to say, increase in the percentage of TDA reduces the stiffness of the samples. In addition, the increase in the percentage of TDA increases the strain that the peak maximum deviatoric stress occurs in. Compared to the results of other TDA mixtures, it seems that the M10 has a higher amount of peak maximum deviatoric stress in all three confining pressures.

Table 5.2 provides the values for cohesion and the angle of internal friction for different mixtures based on Mohr-Coulomb failure criterion. These values were calculated using the ultimate limit state. The table suggests that by adding TDA to gravel, the angle of internal friction decreases while the cohesion increases.

Table 5.2 Values of cohesion and the angle of internal friction

Composition	Cohesion (kPa)	The angle of internal friction (φ)
Gravel	-	49
M5	62	41
M10	68	42
M20	51	42
M30	109	36

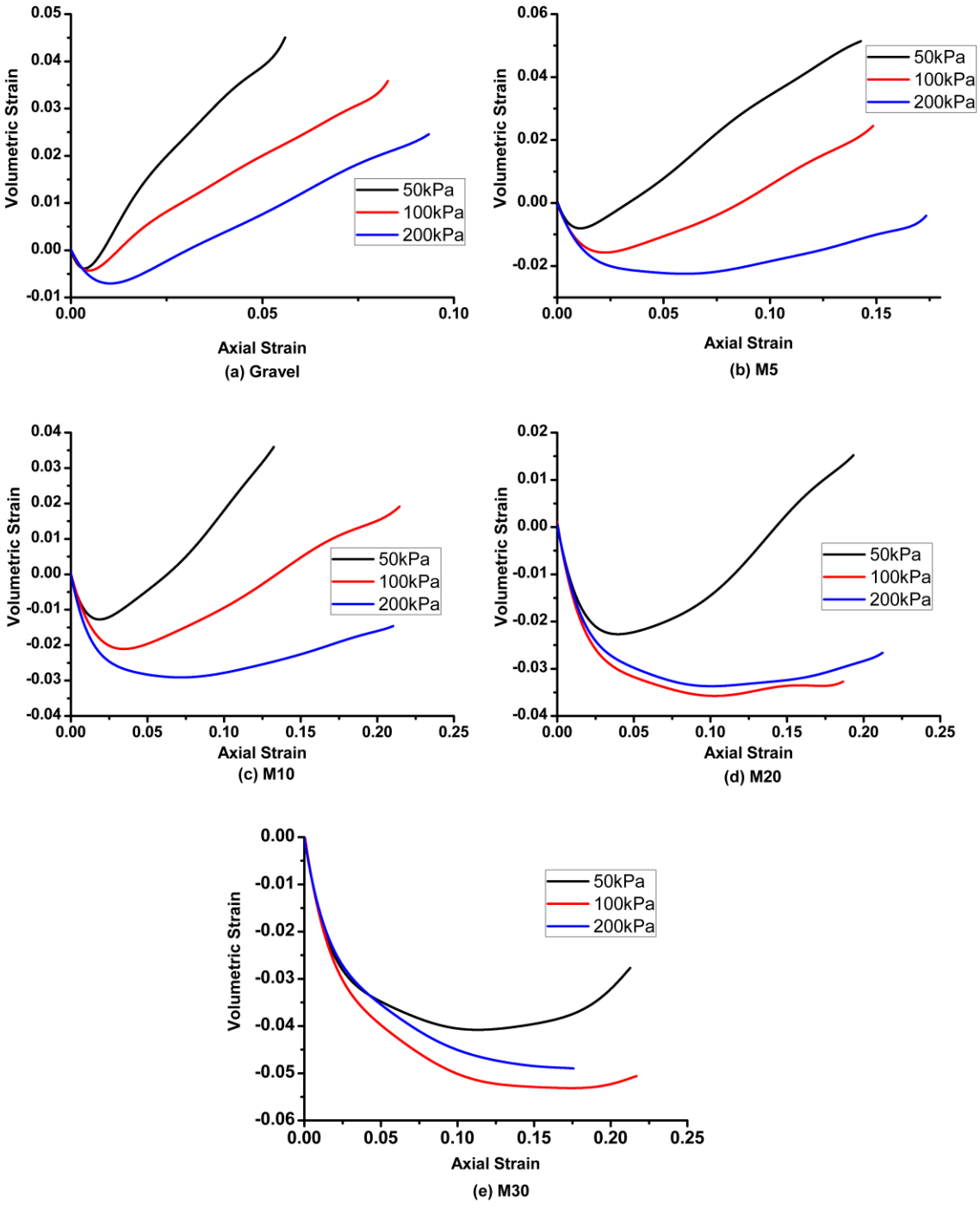

Fig. 5.3 Volumetric strain of the samples

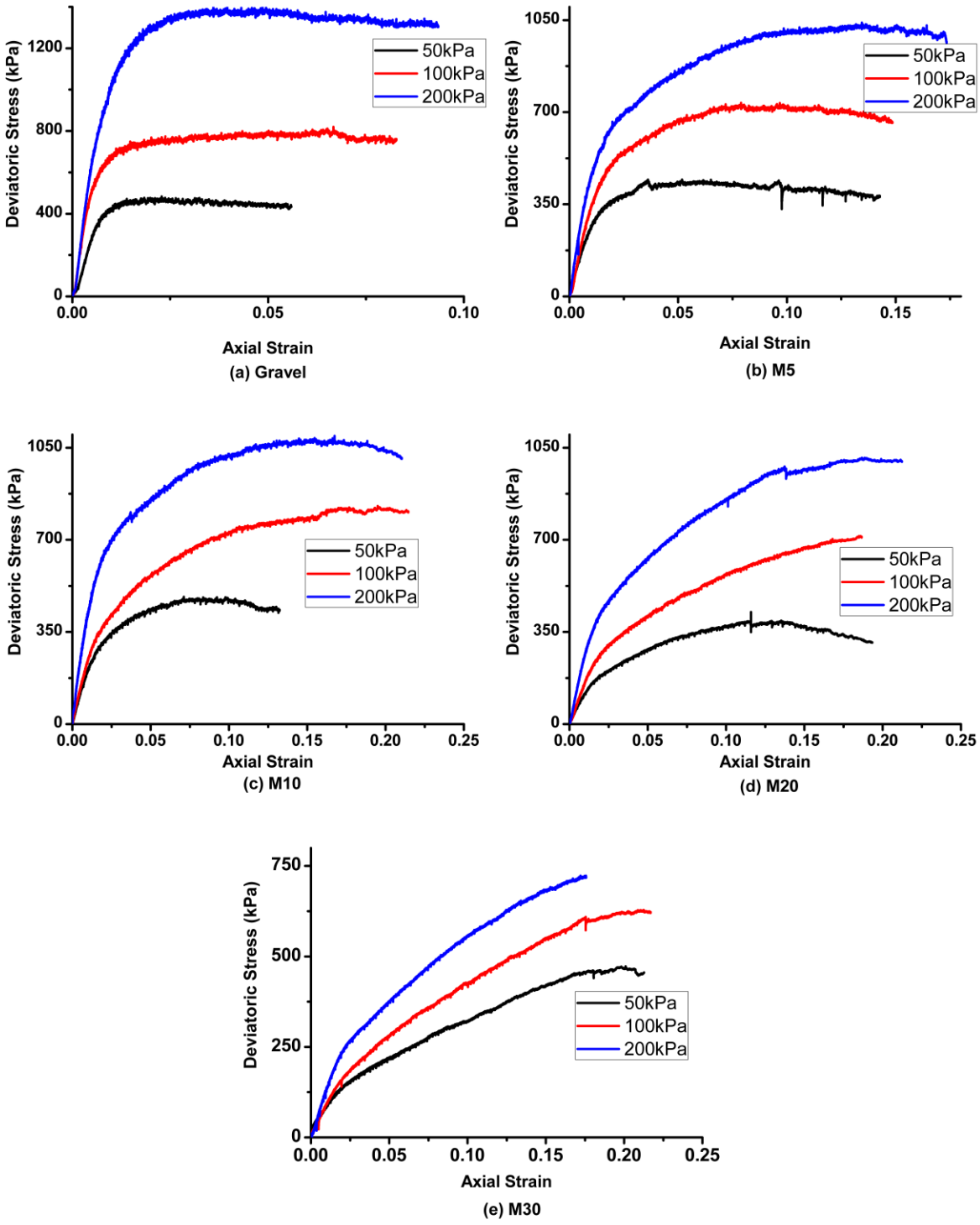

Fig. 5.4 Deviatoric stress vs. strain for each composition

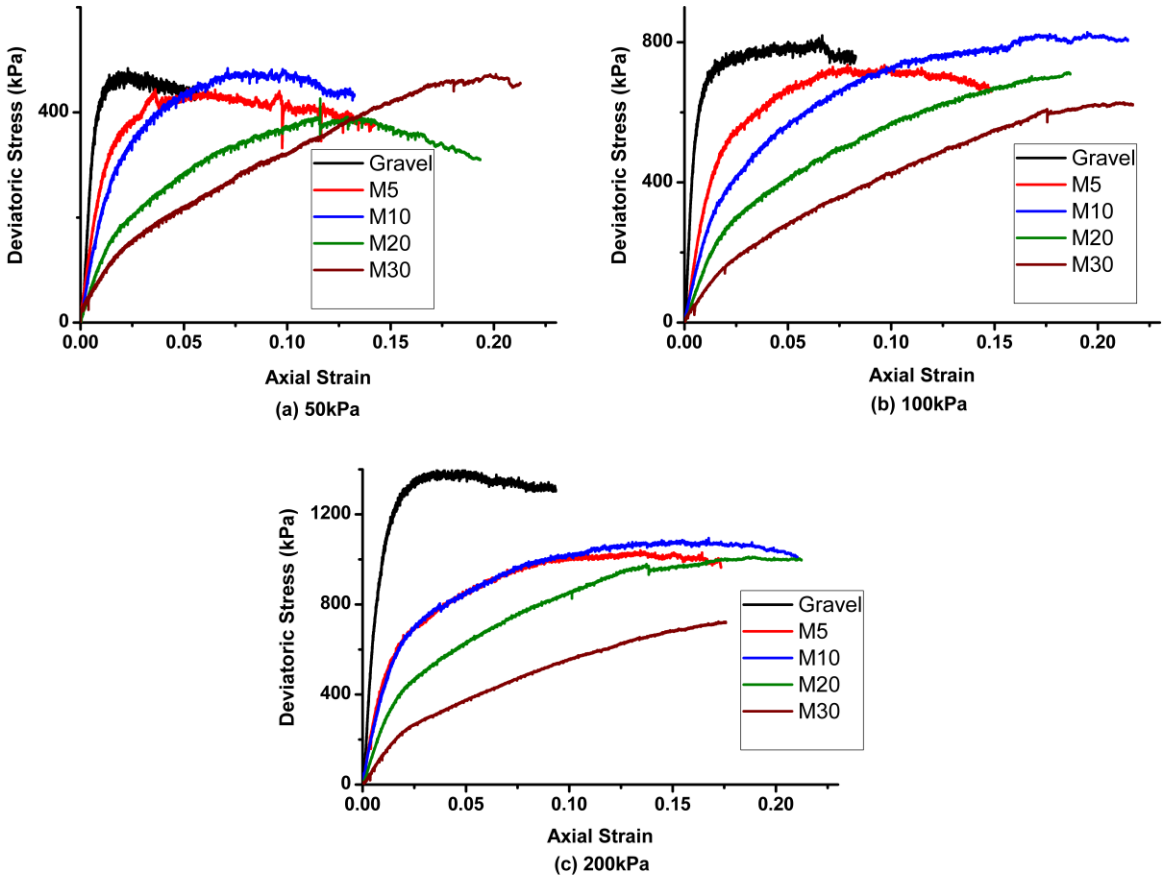

Fig. 5.5 Comparison of deviatoric stress vs. strain in each confining pressure

5.7 CONCLUSIONS

In this study a series of triaxial tests were performed on different mixture compositions of TDA and gravel. The gravel used in this study was type 1 gravel per Nova Scotia Transportation and Public Works Standard Specification. The TDA used in the study was TDA type A per ASTM D6270-08 which is the size used in most civil engineering projects. Sample sets were prepared with varying percentages of TDA. Each sample set was tested in three different confining pressures, and the results of deviatoric stress and volumetric strain versus axial strain were depicted. Finally, the values of cohesion and the

angle of internal friction for each mixture composition were presented. Based on the results of the conducted testing program, the following conclusions can be drawn:

- As the percentage of TDA in content increases, the volumetric strain of the samples changes its behaviour;
- Increase in the percentage of TDA leads to increases in the strain that the maximum stress occurs at;
- The sample with 10% TDA exhibits higher amounts of maximum deviatoric stress compared to the other TDA mixtures;
- Samples with lower amounts of TDA have higher strength compared to samples with higher amounts of TDA;
- Adding TDA to gravel increases the cohesion while decreases the angle of internal friction.

ACKNOWLEDGEMENTS

The authors acknowledge the financial support provided by the Natural Sciences and Engineering Council of Canada (NSERC), and the generosity of our research collaborator Halifax C&D Recycling Limited for the donation of all the TDA materials used in this project.

REFERENCES

Ashari, M., El Naggar, H., & Martins, Y. (2017). Evaluation of the physical properties of TDA-sand mixtures. In *GeoOttawa 2017*.

El Naggar, H., Soleimani, P., & Fakhroo, A. (2016). Strength and Stiffness Properties of Green Lightweight Fill Mixtures. *Geotechnical and Geological Engineering*, *34*(3), 867–876. https://doi.org/10.1007/s10706-016-0010-1

Foose, G. J., Benson, C. H., & Bosscher, P. J. (1996). Sand Reinforced with Shredded Waste Tires. *Journal of Geotechnical Engineering*, *122*(9), 760–767. https://doi.org/10.1061/(ASCE)0733-9410(1996)122:9(760)

Lee, J. H., Salgado, R., Bernal, A., & Lovell, C. W. (1999). Shredded Tires and Rubber-Sand as Lightweight Backfill. *Journal of Geotechnical and Geoenvironmental Engineering*, *125*(February), 132–141.

Masad, E., Taha, R., Ho, C., & Papagiannakis, T. (1996). Engineering Properties of Tire / Soil Mixtures as a Lightweight Fill Material. *Geotechnical Testing Journal, 19*, 297–304. https://doi.org/10.1520/GTJ10355J

Noorzad, R., & Raveshi, M. (2017). Mechanical Behavior of Waste Tire Crumbs–Sand Mixtures Determined by Triaxial Tests. *Geotechnical and Geological Engineering*, *35*(4), 1793–1802. https://doi.org/10.1007/s10706-017-0209-9

Rubber manufacturers association. (2016). 2015 U . S . Scrap Tire Management Summary U . S . Scrap Tire Disposition 2015, (May 2016), 1–19.

Tatlisoz, N., Edil, T. B., & Benson, C. H. (1998). Interaction between Reinforcing Geosynthetics and Soil-Tire Chip Mixtures. *Journal of Geotechnical and Geoenvironmental Engineering*, *124*(11), 1109–1119. https://doi.org/10.1061/(ASCE)1090-0241(1998)124:11(1109)

Zalando. (2016). Annual Report 2016. *Zalando Corporate Website*, 175. https://doi.org/10.1017/CBO9781107415324.004

Zornberg, J. G., Cabral, A. R., & Viratjandr, C. (2004). Behaviour of tire shred - sand mixtures. *Canadian Geotechnical Journal*, *41*(2), 227–241. https://doi.org/10.1139/t03-086

CHAPTER 6 COMPARISON BETWEEN THE PERFORMANCE OF CONSIDERED BACKFILLING OPTIONS

In this chapter, empirical equations are provided for TDA mixtures with sand and gravel. Then two conventional backfilling materials, i.e. sand and gravel, are compared to three emerging backfilling alternatives, i.e. TDA, TDA/sand mixture and TDA/gravel mixture in terms of strength parameters and stiffness. Finally, a construction guideline is proposed for the overbuild needed to achieve a desired thickness layer of the mixtures in the field.

6.1 EMPIRICAL EQUATIONS

This section presents empirical equations derived from the results of tests conducted on mixtures of TDA and sand or gravel which were discussed in chapters 4 and 5. To find the regression method which best suits the laboratory results, advanced regression methods were tested. The equation with two exponential terms achieved the highest amounts of R^2 when representing the amount of deviatoric stress in relation to strain, confining pressure and the ratio of TDA in the mixture by weight.

The equation below is the general format for the empirical equations:

$$\sigma(\varepsilon, \sigma_3) = (a\sigma_3 + b)e^{\frac{-f\varepsilon}{100}} - (c\sigma_3 + d)e^{-f\varepsilon} \qquad (6.1)$$

$$E_{tan}(\sigma_3) = f(c\sigma_3 + d) - \frac{f}{100}(a\sigma_3 + b) \qquad (6.2)$$

where σ is deviatoric stress (kPa), σ_3 is the confining pressure (kPa), ε is the amount of axial strain and E_{tan} is the tangent modulus (kPa). The equation for E_{tan} was derived by calculating the derivative of the first equation with respect to ε and then plugging the amount of 0 for ε. The values for a, b, c, d and f were manipulated to achieve the highest

amount of R^2. Table 6.1 represents the values for a to f and the corresponding R^2 for each mixture composition.

Table 6.1 The values for a, b, c, d and f for each mixture composition

	w (ratio of TDA by weight)	a	b	c	d	f	R^2
G5	0.05	3.756	305.2	4.584	180.8	54	0.9564
G10	0.10	3.668	386.4	3.261	411.3	35	0.9612
G20	0.20	4.001	227.6	4.206	190.9	23	0.9738
G30	0.30	2.101	438.9	1.904	440.2	11	0.9806
S15	0.0636	3.688	35.9	4.893	-30.77	200	0.9937
S25	0.1136	2.95	133.8	3.699	81.65	147	0.9863
S50	0.2778	3.602	99.78	4.773	-1.942	60	0.9738
S75	0.5357	5.223	104.3	5.627	36.31	9	0.9896

The equations below predict the values of a, b, c, d and f for gravel and sand mixtures.

For gravel mixtures:

$$a = -582.3w^3 + 237.8w^2 - 27.23w + 4.596$$

$$b = 159700w^3 - 77300w^2 + 10420w - 42.74$$

$$c = -1607w^3 + 801.9w^2 - 118.6w + 8.711$$

$$d = 275600w^3 - 141900w^2 + 21070w - 552.5$$

$$f = -6933w^3 + 4160w^2 - 882.7w + 88.6$$

For sand mixtures:

$$a = -173.6w^3 + 166.4w^2 - 40.06w + 5.607$$

$$b = 22540w^3 - 20360w^2 + 5022w - 206.9$$

$$c = -317w^3 + 286.3w^2 - 66.94w + 8.074$$

$$d = 30570w^3 - 26780w^2 + 6255w - 328.1$$

$$f = 970.9w^2 - 974.2w + 252.8$$

Fig. 6.1 to 6.8 compare the results of the empirical equations proposed in this chapter to the results obtained in the laboratory. These figures show a strong agreement between the proposed empirical equations and the obtained laboratory results.

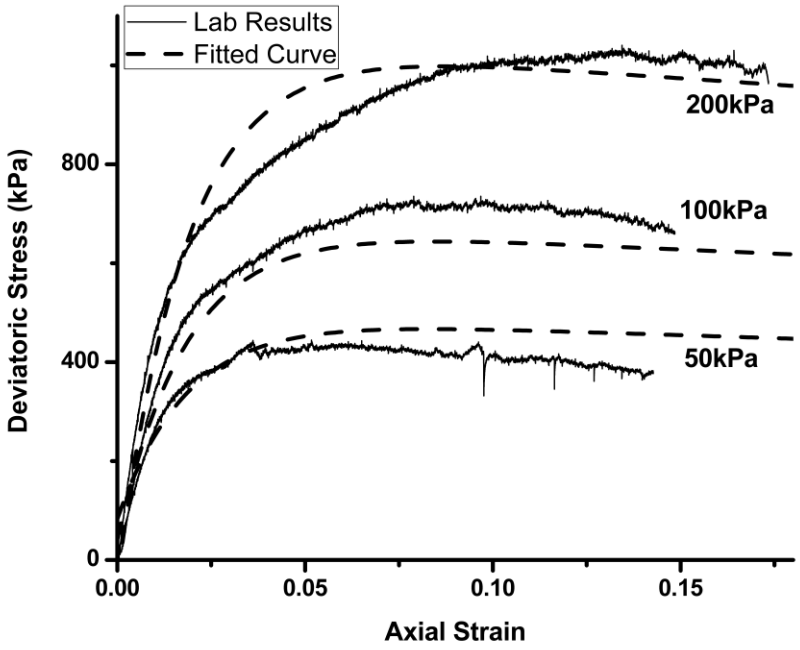

Fig. 6.1 Comparison between the laboratory results and the empirical equation (G5)

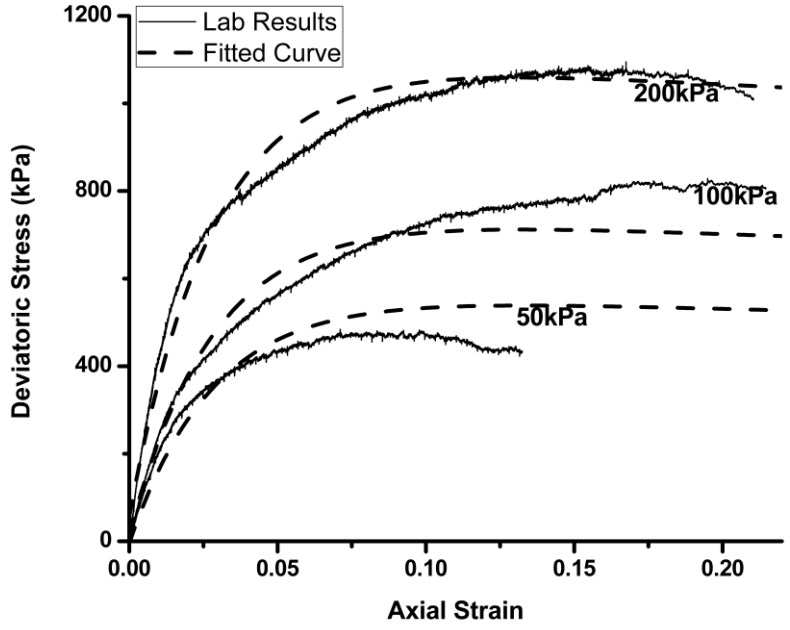

Fig. 6.2 Comparison between the laboratory results and the empirical equation (G10)

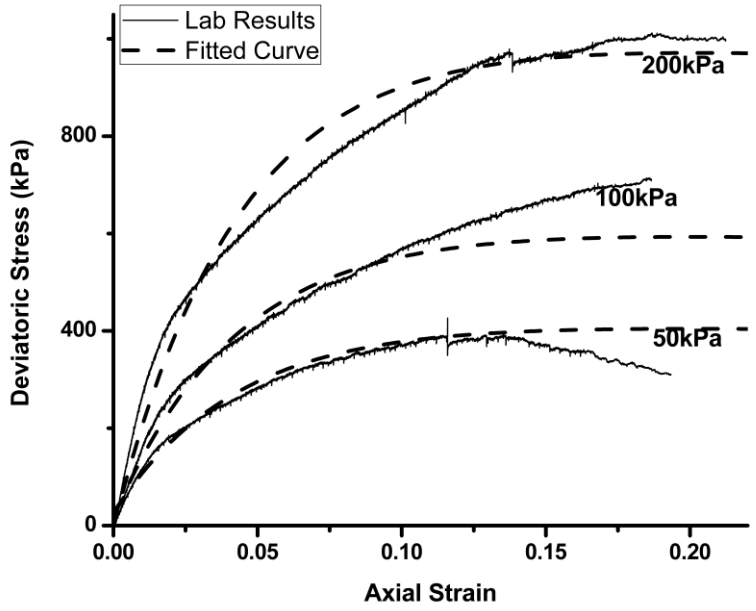

Fig. 6.3 Comparison between the laboratory results and the empirical equation (G20)

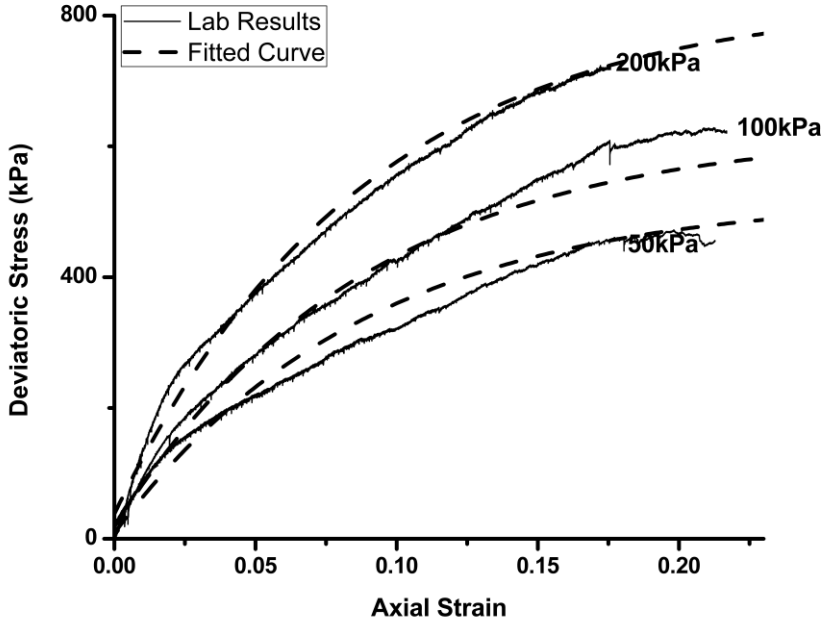

Fig. 6.4 Comparison between the laboratory results and the empirical equation (G30)

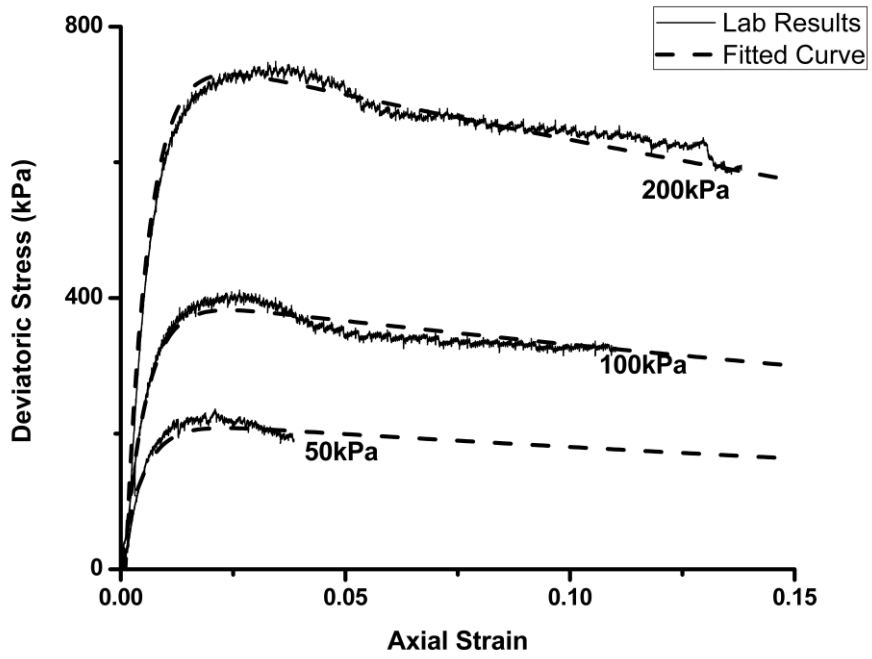

Fig. 6.5 Comparison between the laboratory results and the empirical equation (S15)

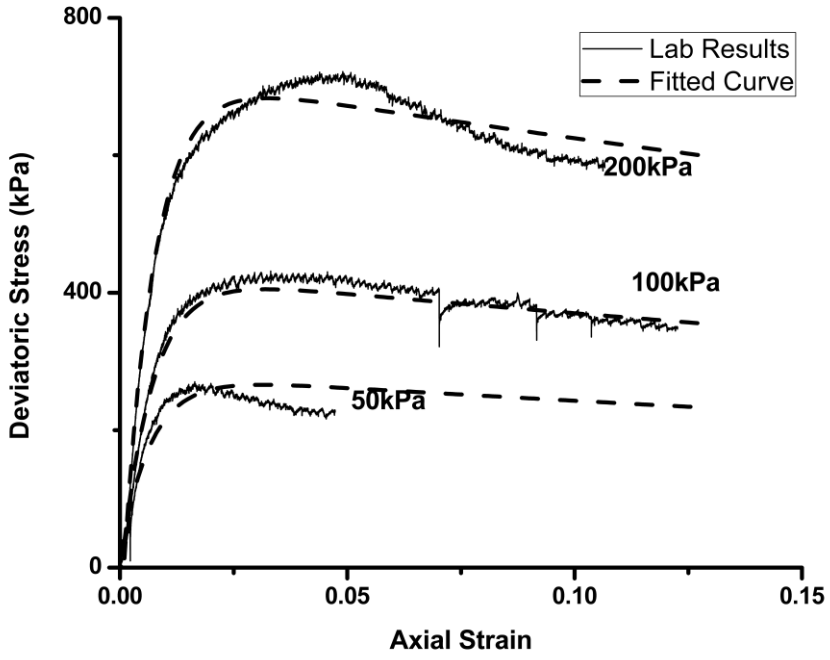

Fig. 6.6 Comparison between the laboratory results and the empirical equation (S25)

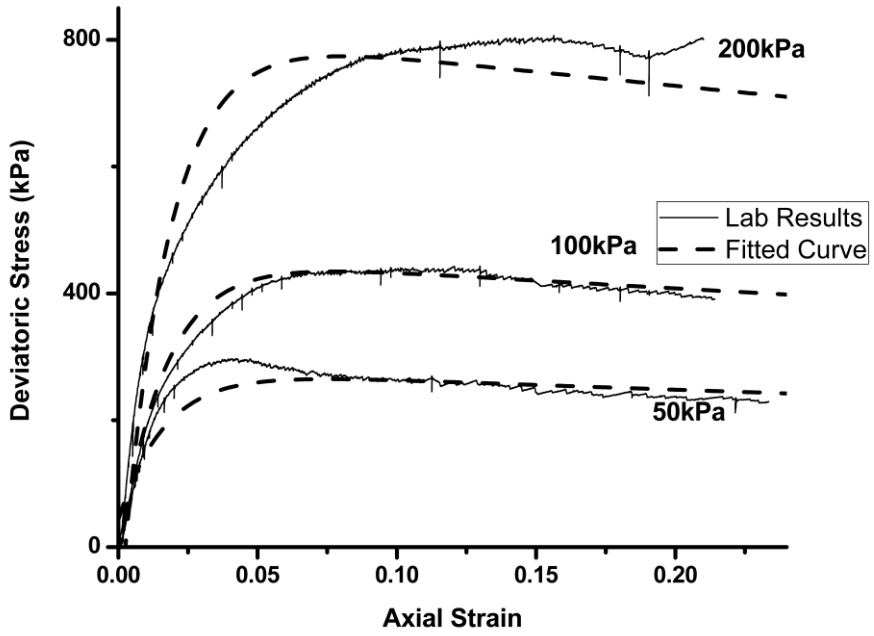

Fig. 6.7 Comparison between the laboratory results and the empirical equation (S50)

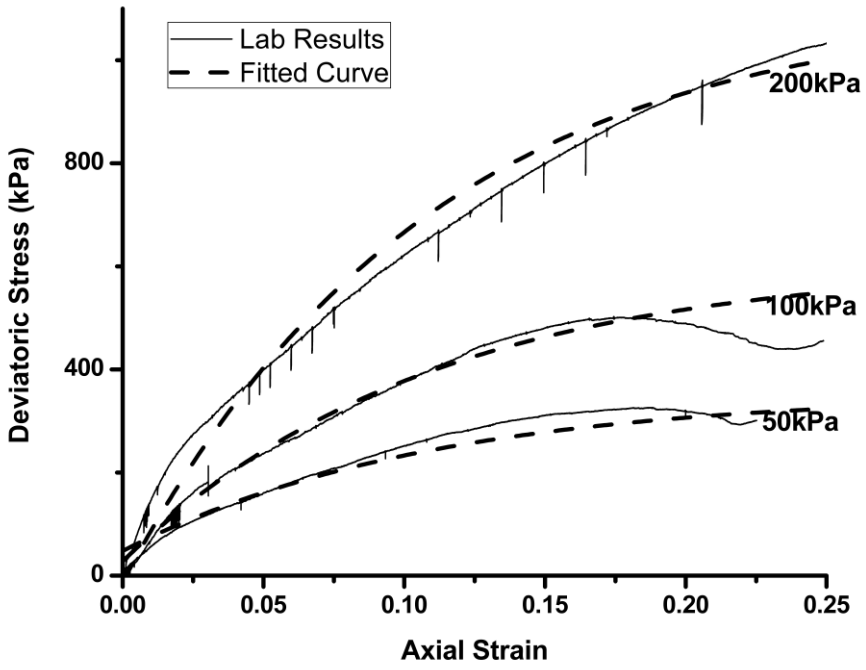

Fig. 6.8 Comparison between the laboratory results and the empirical equation (S75)

6.2 STRENGTH PARAMETERS

Table 6.2 compares the values of cohesion and the angle of internal friction for all the materials tested in this research. In cases where the test did not reach a conclusive peak for deviatoric stress, according to ASTM D7181-11, the stress at 15% strain was used to calculate the values of cohesion and the angle of internal friction.

Table 6.2 Comparison between the strength parameters

Material	TDA % by weight	Cohesion (kPa)	Angle of internal friction (°)	Dry density (kg/m^3)
TDA	100	23.5	25.5	710
Gravel	0	-	49	2108
G5	5	62	41	1815
G10	10	68	42	1749
G20	20	51	42	1593
G30	30	109	36	1483
Sand	0	-	39	1717
S15	6.36	15.4	39	1705
S25	11.36	29.7	38	1683
S50	27.78	32.3	39	1569
S75	53.57	36	40	1261

Designers usually consider a combination of availability, strength parameters, dry density, stiffness and cost to come up with the most suitable material for their designs. While the strength and stiffness of pure TDA compared to pure sand or gravel is lower, the lower density of TDA can make pure TDA a better choice for some applications, e.g. backfilling material for embankments on soft soils. The same can be said about mixtures of TDA and sand and gravel. As the percentage of TDA increases in the mixtures of sand and TDA, the angle of internal friction remains constant, but the amount of cohesion increases and at the same time the dry density of the composition decreases. These changes make the TDA/sand mixture a better backfilling material in many applications. The same cannot be said for mixtures of gravel and TDA. Pure gravel has a higher amount of angle of internal friction compared to its mixtures with TDA. However, as it is shown in Fig. 5.5, compared to G10, pure gravel has approximately the same amount of maximum deviatoric stress for confining pressures of 50 and 100 kPa and a lower amount of maximum deviatoric stress for the confining pressure of 200 kPa. The equivalent performance of G10 in lower confining pressures mixed with its lower dry density makes G10 a very good alternative to pure gravel in shallower backfilling layers which is commonly needed.

6.3 STIFFNESS

To compare the stiffness of the materials used in this research, the values for E_{50} (secant modulus) were calculated for each mixture of gravel and sand with TDA and depicted in Fig. 6.9 and 6.10.

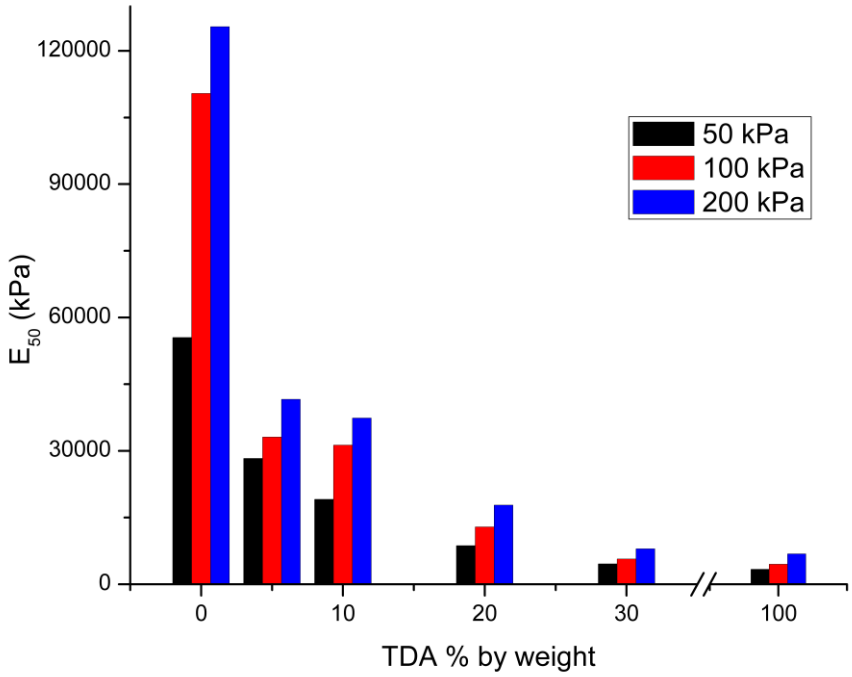

Fig. 6.9 E_{50} for different mixtures of gravel and TDA

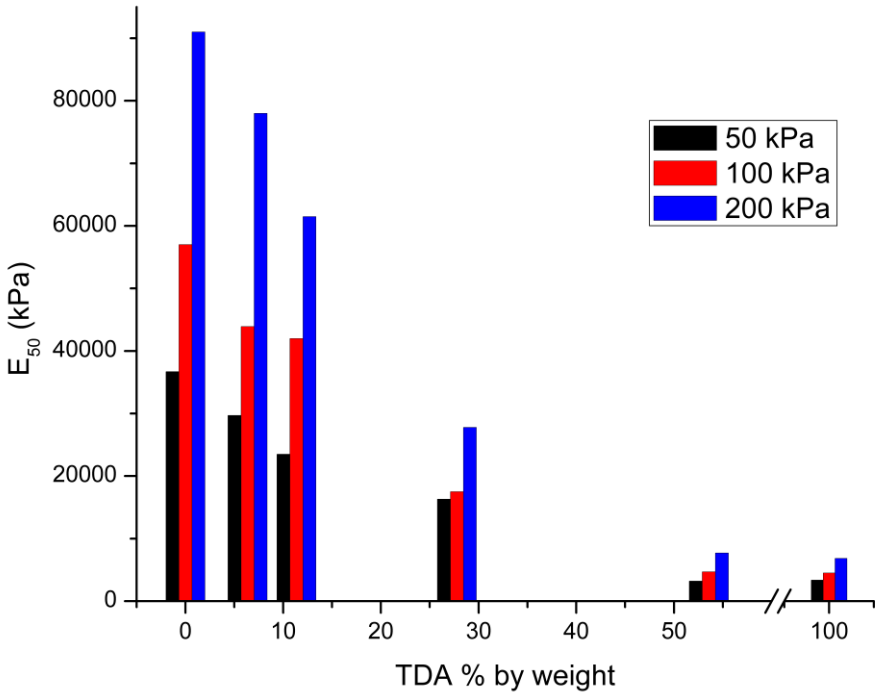

Fig. 6.10 E_{50} for different mixtures of sand and TDA

As it is evident from the figures, adding TDA to gravel or sand, decreases the amount of secant modulus. This decrease occurs at higher rates for mixtures of gravel and TDA. For example, adding small amounts of TDA to gravel has a huge effect on the amount of secant modulus of gravel mixtures (an average of 65% decrease in the E_{50} for adding 5% TDA by weight). Adding almost the same amount of TDA to sand, the effect is less noticeable (an average of 18% decrease in the E_{50} for adding 6.36% TDA by weight). This difference in the behaviour of the two mixtures can be related to the difference in sand and gravel particle sizes. The smaller particle size in sand compared to gravel, can fill the voids in the mixture efficiently which makes the behaviour of sand mixtures closer to the behaviour of pure sand. On the other hand, the larger particle size of gravel makes it hard for gravel particles to fill the voids. This can be observed in the sudden plunge in the dry density of gravel. By introducing 5% TDA by weight to gravel, the gravel mixture loses almost 14% of its dry density. Adding almost the same amount of TDA to sand (6.36% by weight), the sand mixture loses less than 1% of its dry density. The extra empty voids can be filled during axial loading which decreases the stiffness of the samples.

6.4 MIXTURE OVERBUILD GUIDELINES

The amount of overbuild needed for a layer of TDA was discussed in chapter 3. Using the same assumptions and methods, the equations below are proposed to calculate the amount of overbuild needed to reach the desired layer thickness:

$$Overbuild = (desired\ layer\ thickness) \times \left(\frac{VP}{100 - VP}\right)$$

where VP is the percentage of volume change. The unit for $Overbuild$ will be the same as the unit used for the $desired\ layer\ thickness$. The equation below predicts the amount of VP for different confining pressures and TDA content for mixtures of TDA with gravel or sand.

For gravel mixtures:

$$VP = 4.928 - 25.04w + .07253\sigma_e w + 96.8w^2$$

For sand mixtures:

$$VP = 0.5737 + 25.72w + .05448\sigma_e w - 30.27w^2$$

where w is the ratio of the weight of the TDA to the weight of the mixture ($0 \leq w \leq 1$) and σ_e is the effective stress of the layer. The above equations are based on the water loss after the consolidation stage during triaxial tests. The coefficients of determination R^2 for the above equations are 0.9702 and 0.9795 respectively.

CHAPTER 7 CONCLUSION

7.1 SUMMARY

This thesis addressed the feasibility of using TDA and mixtures of TDA and sand or gravel as an alternative backfilling material. Over the course of the research, consolidated drained triaxial tests were performed on different samples of TDA and TDA mixtures. The results of these tests were discussed, and empirical equations were derived. Below is the description of each chapter.

The first chapter outlines the problem that this thesis is addressing and describes the research objectives. This chapter also includes a description of the methodology of this research.

The second chapter consists of a literature review of research conducted on TDA. In this chapter, different tests on TDA and its compositions were reviewed, and advantages and disadvantages of each test method were reported. Test methods discussed included: field tests, direct shear tests, triaxial tests and other laboratory tests. For each of these test methods, a concise table comparing previous research was included.

The third chapter contains a description of the triaxial tests conducted on TDA as part of this research. The values for deviatoric stress vs. strain of TDA under different confining pressures were evaluated. The equations that best fit these values were presented. Based on these values, the strength parameters of TDA were calculated. Finally, an overbuild guideline for determining the thickness of TDA layers in the field was presented.

In the fourth chapter, triaxial tests were conducted on five different compositions of TDA and sand. For each composition, three confining pressures were tested. Based on the test results, the geotechnical properties of TDA mixtures with sand were evaluated. The results of these tests were compared and discussed.

Similar to the fourth chapter, the fifth chapter describes triaxial tests conducted on five different compositions of TDA and gravel mixtures. Each composition was subjected to three different confining pressures. The results were used to evaluate the geotechnical properties of TDA mixtures with gravel.

In the sixth chapter, the results of chapters three, four and five were compared. Empirical equations were proposed to predict the laboratory results for mixtures of TDA and gravel or sand. The empirical equations were compared to the laboratory results to determine their accuracy. The values of E_{50} for each mixture composition were calculated and compared. Finally, guidelines for the amount of overbuild needed in the field for layers containing TDA mixtures were proposed.

7.2 TDA RESULTS

- Percentage of volume change in the TDA samples subjected only to confining pressure can be calculated using:

$$VP = 3.12\sigma_3^{0.39};$$

- The changes in volume that occurred during axial loading had no meaningful relationship with confining pressure applied;

- While the deviatoric stress vs. strain curves for small particle size TDA with no steel present reported by other researchers showed a linear trend, this research displayed that this trend is nonlinear for TDA Type A;
- The amount of deviatoric stress vs. strain and secant modulus for TDA Type A can be calculated by these equations:

$$\sigma(\varepsilon, \sigma_3) = \varepsilon[(21\sigma_3 + 2470)e^{-28.9\varepsilon} + (17.4\sigma_3 + 698)e^{-3.78\varepsilon}],$$

$$E_{50}(\varepsilon, \sigma_3) = (7.982\sigma_3 + 778.8)e^{\left(-168.5\sigma_3^{-.03866} + 98.8\right)\varepsilon} +$$

$$(30.23\sigma_3 + 2416)e^{\left(4.105\sigma_3^{-.3318} - 2.129\right)\varepsilon}$$

- The strength parameters of TDA Type A can be evaluated for different maximum strains allowed using the equations below:

$$\varphi(\varepsilon) = \frac{31\varepsilon}{\varepsilon + .032}$$

$$c(\varepsilon) = \frac{26\varepsilon}{\varepsilon + .016}$$

- To calculate the amount of overbuild needed to reach the desired thickness for a TDA layer in the field, equation below can be used:

$$Overbuild = (TDA\ layer\ thickness) \times \left(\frac{3.12\sigma_e^{0.39}}{100 - 3.12\sigma_e^{0.39}}\right)$$

7.3 MIXTURES OF TDA AND SOIL

- As the percentage of TDA increases, the behaviour of volumetric strain in the mixtures shifts from resembling soil to resembling TDA;

- The same trend of shift from soil to TDA is true for deviatoric stress versus strain curves;
- For low TDA content in mixtures of TDA and sand, the changes in dry density are minimal. In contrast, low TDA content in mixtures of gravel and TDA results in a huge drop in the dry density of the mixtures;
- Similar to changes in dry density, low TDA content has a more significant effect on strength parameters and stiffness of TDA mixtures with gravel compared to TDA mixtures with sand;
- The deviatoric stress versus strain can be calculated using the equations below:

$$\sigma(\varepsilon, \sigma_3) = (a\sigma_3 + b)e^{\frac{-f\varepsilon}{100}} - (c\sigma_3 + d)e^{-f\varepsilon}$$

- The values of a, b, c, d and f for the above equation can be calculated for mixtures of TDA and sand using:

$$a = -582.3w^3 + 237.8w^2 - 27.23w + 4.596$$

$$b = 159700w^3 - 77300w^2 + 10420w - 42.74$$

$$c = -1607w^3 + 801.9w^2 - 118.6w + 8.711$$

$$d = 275600w^3 - 141900w^2 + 21070w - 552.5$$

$$f = -6933w^3 + 4160w^2 - 882.7w + 88.6$$

- The values of a, b, c, d and f for mixtures of TDA and gravel can be calculated using:

$$a = -173.6w^3 + 166.4w^2 - 40.06w + 5.607$$

$$b = 22540w^3 - 20360w^2 + 5022w - 206.9$$

$$c = -317w^3 + 286.3w^2 - 66.94w + 8.074$$

$$d = 30570w^3 - 26780w^2 + 6255w - 328.1$$

$$f = 970.9w^2 - 974.2w + 252.8$$

- The amount of over build needed to reach a desired thickness layer in the field can be calculated using:

$$Overbuild = (desired\ layer\ thickness) \times \left(\frac{VP}{100 - VP}\right)$$

- The value of VP in the above equation for mixtures of gravel and TDA can be calculated using:

$$VP = 4.928 - 25.04w + .07253\sigma_e w + 96.8w^2$$

- The value of VP for mixtures of sand and TDA can be calculated using:

$$VP = 0.5737 + 25.72w + .05448\sigma_e w - 30.27w^2$$

7.4 RECOMMENDATIONS

The following suggestions are recommended for further investigations in order to gain a better understanding of civil engineering applications of TDA.

- Testing larger size TDA Type B to evaluate its engineering properties and its advantages/disadvantages over TDA Type A;
- Performing laboratory tests on TDA mixed with other types of soil to have a more inclusive library of engineering properties of TDA mixtures;

- Performing tests on large size TDA, to evaluate its Poisson's ratio and lateral earth pressure values.
- Performing other types of laboratory tests on TDA, especially dynamic tests to analyze the dynamic behaviour of TDA.

REFERENCES

Ahn, I. S., & Cheng, L. (2014). Tire derived aggregate for retaining wall backfill under earthquake loading. *Construction and Building Materials*, *57*, 105–116. https://doi.org/10.1016/j.conbuildmat.2014.01.091

Aliabdo, A. A., Abd Elmoaty, A. E. M., & Abdelbaset, M. M. (2015). Utilization of waste rubber in non-structural applications. *Construction and Building Materials*, *91*, 195–207. https://doi.org/10.1016/j.conbuildmat.2015.05.080

Arroyo, M., Estaire, J., Sanmartin, I., & Lloret, A. (2008). Size effect on tire derived aggregate mechanical properties. *Proceedings of the International Workshop on Scrap Tire Derived Geomaterials - Opportunities and Challenges, IW-TDGM 2007*, 151–160. Retrieved from http://www.scopus.com/inward/record.url?eid=2-s2.0-60749107484&partnerID=tZOtx3y1

Ashari, M., El Naggar, H., & Martins, Y. (2017). Evaluation of the physical properties of TDA-sand mixtures. In *GeoOttawa 2017*.

Azevedo, F., Pacheco-Torgal, F., Jesus, C., Barroso De Aguiar, J. L., & Camões, A. F. (2012). Properties and durability of HPC with tyre rubber wastes. *Construction and Building Materials*, *34*, 186–191. https://doi.org/10.1016/j.conbuildmat.2012.02.062

Bali Reddy, S., Pradeep Kumar, D., & Murali Krishna, A. (2015). Evaluation of the Optimum Mixing Ratio of a Sand-Tire Chips Mixture for Geoengineering Applications. *Journal of Materials in Civil Engineering*, *28*(2), 6015007. https://doi.org/10.1061/(ASCE)MT.1943-5533.0001335

Cetin, H., Fener, M., & Gunaydin, O. (2006). Geotechnical properties of tire-cohesive clayey soil mixtures as a fill material. *Engineering Geology*, *88*(1–2), 110–120. https://doi.org/10.1016/j.enggeo.2006.09.002

Eaton, R. A., Roberts, R. J., & Humphrey, D. N. (1994). Gravel Road Test Sections Insulated with Scrap Tire Chips Construction and First Year â€™ s Results aC a, (August).

Edinçliler, A., Baykal, G., & Saygili, A. (2010). Influence of different processing techniques on the mechanical properties of used tires in embankment construction. *Waste Management*, *30*(6), 1073–1080. https://doi.org/10.1016/j.wasman.2009.09.031

El Naggar, H., Soleimani, P., & Fakhroo, A. (2016). Strength and Stiffness Properties of Green Lightweight Fill Mixtures. *Geotechnical and Geological Engineering*, *34*(3), 867–876. https://doi.org/10.1007/s10706-016-0010-1

Foose, G. J., Benson, C. H., & Bosscher, P. J. (1996). Sand Reinforced with Shredded Waste Tires. *Journal of Geotechnical Engineering*, *122*(9), 760–767. https://doi.org/10.1061/(ASCE)0733-9410(1996)122:9(760)

Hataf, N., & Rahimi, M. M. (2006). Experimental investigation of bearing capacity of sand reinforced with randomly distributed tire shreds. *Construction and Building Materials*, *20*(10), 910–916. https://doi.org/10.1016/j.conbuildmat.2005.06.019

Kim, Y. T., & Kang, H. S. (2011). Engineering Characteristics of Rubber-Added Lightweight Soil as a Flowable Backfill Material. *Journal of Materials in Civil Engineering*, *23*(9), 1289–1294. https://doi.org/10.1061/(ASCE)MT.1943-5533.0000307

Kowalska, M. (2016). Compactness of Scrap Tyre Rubber Aggregates in Standard Proctor Test. *Procedia Engineering*, *161*, 975–979. https://doi.org/10.1016/j.proeng.2016.08.836

Lee, C., Shin, H., & Lee, J.-S. (2014). Behavior of sand-rubber particle mixtures: experimental observations and numerical simulations. *International Journal for Numerical and Analytical Methods in Geomechanics*, *38*(16), 1651–1663. https://doi.org/10.1002/nag.2264

Lee, H. J., & Roh, H. S. (2007). The use of recycled tire chips to minimize dynamic earth pressure during compaction of backfill. *Construction and Building Materials*, *21*(5), 1016–1026. https://doi.org/10.1016/j.conbuildmat.2006.02.003

Lee, J. H., Salgado, R., Bernal, A., & Lovell, C. W. (1999). Shredded Tires and Rubber-Sand as Lightweight Backfill. *Journal of Geotechnical and Geoenvironmental Engineering*, *125*(February), 132–141.

Masad, E., Taha, R., Ho, C., & Papagiannakis, T. (1996). Engineering Properties of Tire / Soil Mixtures as a Lightweight Fill Material. *Geotechnical Testing Journal, 19*, 297–304. https://doi.org/10.1520/GTJ10355J

Meles, D., Bayat, A., & Chan, D. (2014). One-dimensional compression model for tire-derived aggregate using large-scale testing apparatus. *International Journal of Geotechnical Engineering*, *8*(2), 197–204. https://doi.org/10.1179/1939787913Y.0000000019

Moo-young, H., Sellasie, K., Zeroka, D., & Sabnis, G. (2003). Physical and Chemical Properties of Recycled Tire Shreds for Use in Construction, *129*(4), 921–929.

Najim, K. B., & Hall, M. R. (2010). A review of the fresh/hardened properties and applications for plain- (PRC) and self-compacting rubberised concrete (SCRC). *Construction and Building Materials*, *24*(11), 2043–2051. https://doi.org/10.1016/j.conbuildmat.2010.04.056

Noorzad, R., & Raveshi, M. (2017). Mechanical Behavior of Waste Tire Crumbs–Sand Mixtures Determined by Triaxial Tests. *Geotechnical and Geological Engineering*, *35*(4), 1793–1802. https://doi.org/10.1007/s10706-017-0209-9

Rubber manufacturers association. (2016). 2015 U . S . Scrap Tire Management Summary U . S . Scrap Tire Disposition 2015, (May 2016), 1–19.

Shalaby, A., & Khan, R. A. (2005). Design of unsurfaced roads constructed with large-size shredded rubber tires: A case study. *Resources, Conservation and Recycling*, *44*(4), 318–332. https://doi.org/10.1016/j.resconrec.2004.12.004

Tatlisoz, N., Edil, T. B., & Benson, C. H. (1998). Interaction between Reinforcing Geosynthetics and Soil-Tire Chip Mixtures. *Journal of Geotechnical and Geoenvironmental Engineering*, *124*(11), 1109–1119. https://doi.org/10.1061/(ASCE)1090-0241(1998)124:11(1109)

Tweedie, J. J., Humphrey, D. N., & Stanford, T. C. (1998). Tire Shreds as Lightweight Retaining Wall Backfill: Active Conditions. *Journal of Geotechnical and Geoenvironmental Engineering*, *124*(November), 1061–1070.

Warith, M. A., Evgin, E., & Benson, P. A. S. (2004). Suitability of shredded tires for use in landfill leachate collection systems. *Waste Management*, *24*(10), 967–979. https://doi.org/10.1016/j.wasman.2004.08.004

Warith, M. A., & Rao, S. M. (2006). Predicting the compressibility behaviour of tire shred samples for landfill applications. *Waste Management*, *26*(3), 268–276. https://doi.org/10.1016/j.wasman.2005.04.011

Wartman, J., Natale, M. F., & Strenk, P. M. (2007). Immediate and Time-Dependent Compression of Tire Derived Aggregate. *Journal of Geotechnical and Geoenvironmental Engineering*, *133*(3), 245–256. https://doi.org/10.1061/(ASCE)1090-0241(2007)133:3(245)

Wu, W. Y., Benda, C. C., & Cauley, R. F. (1997). Triaxial Determination of Shear Strength of Tire Chips. *Journal of Geotechnical and Geoenvironmental Engineering*, *123*(5), 479–482. https://doi.org/10.1061/(ASCE)1090-0241(1997)123:5(479)

Xiao, M., Ledezma, M., & Hartman, C. (2013). Shear resistance of tire derived aggregate (TDA) using large-scale direct shear tests. *Journal of Materials in Civil Engineering*, *0*(ja). https://doi.org/doi:10.1061/(ASCE)MT.1943-5533.0001007

Yi, Y., Meles, D., Nassiri, S., & Bayat, A. (2015). On the compressibility of tire-derived aggregate : comparison of results from laboratory and field tests, *458*(August 2014), 442–458.

Yoon, S., Prezzi, M., Siddiki, N. Z., & Kim, B. (2006). Construction of a test embankment using a sand-tire shred mixture as fill material. *Waste Management*, *26*(9), 1033–1044. https://doi.org/10.1016/j.wasman.2005.10.009

Youwai, S., & Bergado, D. T. (2003). Strength and deformation characteristics of shredded rubber tire - sand mixtures. *Canadian Geotechnical Journal*, *40*(2), 254–264. https://doi.org/10.1139/t02-104

Zalando. (2016). Annual Report 2016. *Zalando Corporate Website*, 175. https://doi.org/10.1017/CBO9781107415324.004

Zornberg, J. G., Cabral, A. R., & Viratjandr, C. (2004). Behaviour of tire shred - sand mixtures. *Canadian Geotechnical Journal*, *41*(2), 227–241. https://doi.org/10.1139/t03-086